Acta Mech 226, 1815–1838 (2015)
DOI 10.1007/s00707-014-1293-z

R. Bustamante · K. R. Rajagopal

Solutions of some boundary value problems for a new class of elastic bodies undergoing small strains. Comparison with the predictions of the classical theory of linearized elasticity: Part I. Problems with cylindrical symmetry

Received: 18 July 2014 / Revised: 20 October 2014 / Published online: 27 December 2014

Abstract There is considerable evidence that shows that for a large class of materials the relationship between the stress and the strain is nonlinear even in the range of strain that is considered small enough for the classical linearized theory of elasticity to be applicable (see Saito et al. in Science 300:464–467, 2003; Li et al. in Phys Rev Lett 98:105503, 2007; Talling et al. in Scr Mater 59:669–672, 2008; Withey et al. in Mater Sci Eng A 493:26–32, 2008; Zhang et al. in Scr Mater 60:733–736, 2009). A proper description of the experiments requires an alternative theory which when linearized would allow the possibility of such a nonlinear relationship between the stress and the strain. Recently, such a theory of elastic bodies has been put into place (see Rajagopal in Appl Math 48:279–319, 2003; Bustamante in Proc R Soc A 465:1377–1392, 2009; Rajagopal in Math Mech Solids 16:536–562, 2011). In this paper, we consider a special class of bodies that belong to the new generalization of response relations for elastic bodies that have a nonlinear relationship between the linearized strain and the stress. We use the special class of bodies that exhibit limited small strain to study two boundary value problems, the first concerning the telescopic shearing and inflation of a tube and the second being the extension, inflation and circumferential shearing of a tube. The results that we obtain for the models under consideration are markedly different from the predictions of the classical linearized elastic model with regard to the same boundary value problems.

1 Introduction

Recent experiments on Gum metal and various metallic alloys (see Saito et al. [1], Li et al. [2], Talling et al. [3], Withey et al. [4], Zhang et al. [5] and others) clearly document the need for a model for an elastic body, wherein the relationship between the stress and strain is nonlinear in the small strain range. The current conventional wisdom within the context of classical elasticity theory dictates the use of the linearized elastic model, which would be impotent to describe the experimental results.[1] Other long-standing problems that also point to the inadequacy of the classical linearized elastic model are those, wherein singularities or unacceptably high strains are predicted within the classical linearized theory, for example, problems concerning cracks, notches, inclusions, defects. These inadequacies of the classical linearized elastic model can be overcome by considering the linearization of implicit constitutive models, which have been proposed to describe the elastic response of

[1] There is a similar need in the case of modelling the behaviour of other inelastic materials such as rock and concrete (assuming as a first approximation that they behave as elastic bodies). Such materials clearly show nonlinear behaviour in the small strain range, see, for example, [9–14].

R. Bustamante (✉)
Departamento de Ingeniería Mecánica, Universidad de Chile, Beaucheff 850, Santiago Centro, Santiago, Chile
E-mail: rogbusta@ing.uchile.cl

K. R. Rajagopal
Department of Mechanical Engineering, University of Texas A&M, College Station, TX, USA

bodies by Rajagopal [6,15], and its various sub-classes. Rajagopal [16] has described the nonlinear response observed in Saito et al. [1] with a nonlinear relationship between the linearized strain and the stress that arises out of the linearization of a new class of constitutive relations; such a nonlinear relationship would be an impossibility were we to consider Cauchy elastic bodies or the set of Green elastic bodies (which is a subset of Cauchy elastic bodies,[2] see [20]) and linearized the same. Such a procedure of Cauchy elastic bodies would lead inevitably to the classical linearized elastic body.

A thermodynamic basis for the more general class of elastic bodies has been introduced by Rajagopal and Srinivasa [21,22] and Bridges [23] (see also [6,15]). Several studies of a variety of initial and boundary value problems have been carried out within the context of sub-classes of such models. Bustamante and Rajagopal [24] studied plane problems within the context of such models, and Bustamante and Rajagopal have studied a variety of other problems within the context of various sub-classes of the new class of elastic bodies (see [25,26]). Rajagopal [27] has studied boundary value problems, such as tension, and inhomogeneous deformations such as torsion and circumferential shear. Bustamante [7] studied what could be interpreted as the Green elastic counterpart to the class of models introduced by Rajagopal. In [6], Rajagopal considered the possibility that the Helmholtz potential in non-dissipative solids could depend on both the stress and the deformation gradient.[3]

Studies have been carried out concerning the development of stresses and strains at crack tips by Rajagopal and Walton [29], and Gou et al. [30] with regard to the existence of cracks in brittle elastic solids wherein cracks propagate without the advent of inelastic response. Ortiz-Bernardin et al. [31,32] have studied the stress concentration due to the presence of circular and elliptic holes in the new class of elastic bodies, and Kulvait et al. [33] have studied the state of the stress and strain at the vicinity of the tip of a notch within the new class. Dynamic problems have also been studied within the context of the new class of elastic bodies, but there are few such studies. Recently, wave propagation in such bodies has been considered by, for example, Kannan et al. [34], who studied waves in slabs of a stress power-law material. Kambapalli et al. [35] have studied circumferential stress waves in annular regions for stress power-law materials, and Bustamante and Sfyris [36] have obtained a general exact solution for a 1D bar, and also some numerical solutions for a constitutive equation showing limiting strain behaviour.

The usefulness of implicit elastic bodies to applications to biological models has been addressed in the papers by Freed and Einstein [37] and in the recent book on soft matter, where an extensive discussion of the utility of such bodies has been articulated (see Freed [28]). Criscione and Rajagopal [38] have studied the response of soft materials within the new class of elastic bodies and show that such models can very effectively describe rubber-like materials. They show that such models can capture quite accurately the experimental results available for such bodies such as those of Penn [39]. Bustamante and Rajagopal [40,41] have generalized the new class of elastic bodies to take into account the effect of electrical fields.

The present study is yet another example of the articulation of the utility and the need for the use of the new class of constitutive relations to describe the non-dissipative response of solids. Bridges and Rajagopal [23] have investigated the response of annular domains, both spherical and cylindrical, within a sub-class of the new class of elastic bodies. The study carried out here is within the context of a different sub-class and the boundary value problems are also more general in that we consider the possibilities of circumferential shear and axial stress in the body.

The organization of the paper is as follows: in Sect. 2, some basic relations for the kinematics of deformation, the equilibrium equation and constitutive relations are presented. In Sect. 3, the problem of telescopic shear and inflation of a tube is studied, while in Sect. 4, an analysis of the circumferential shear and inflation of a tube is presented.

2 Basic equations

2.1 Kinematics

Let $\mathbf{X}$, where $\mathbf{X} = \boldsymbol{\kappa}_r(X)$, denote the position of a particle X of a body $\mathcal{B}$ in the reference configuration $\kappa_r(\mathcal{B})$. It is assumed that there exists a one-to-one mapping $\boldsymbol{\chi}$ such that at any time t it assigns the position $\mathbf{x} = \boldsymbol{\chi}(\mathbf{X}, t)$

[2] See [17,18]. Carroll [19] has shown that a Cauchy elastic body that is not Green elastic would lead to a body, which would be an infinite source of energy. This result was anticipated in the seminal work of Green [17,18].

[3] Rajagopal considered the one-dimensional case, when the Helmholtz potential depends on the one-dimensional stress and strain. Recently, Freed [28] has considered three-dimensional models, wherein the Helmholtz potential depends on the stress and the deformation gradient.

to the particle X, in the current configuration $\kappa_t(\mathcal{B})$. The displacement field $\mathbf{u}$ is defined as:

$$\mathbf{u} = \mathbf{x} - \mathbf{X}. \tag{1}$$

The deformation gradient $\mathbf{F}$, the right and left Cauchy-Green deformation tensor $\mathbf{C}, \mathbf{B}$, the Lagrangian Green-St. Venant strain tensor $\mathbf{E}$ and the linearized strain tensor $\boldsymbol{\varepsilon}$ are defined by:

$$\mathbf{F} = \frac{\partial \boldsymbol{\chi}}{\partial \mathbf{F}}, \quad \mathbf{C} = \mathbf{F}^{\mathrm{T}}\mathbf{F}, \quad \mathbf{B} = \mathbf{F}\mathbf{F}^{\mathrm{T}}, \quad \mathbf{E} = \frac{1}{2}(\mathbf{C} - \mathbf{I}), \quad \boldsymbol{\varepsilon} = \frac{1}{2}(\nabla_{\mathbf{X}}\mathbf{u} + \nabla_{\mathbf{X}}\mathbf{u}^{\mathrm{T}}), \tag{2.1–5}$$

where $\nabla_{\mathbf{X}}$ is the gradient operator defined with respect to the reference configuration. We shall henceforth assume that $J = \det \mathbf{F} > 0$. For more details about the kinematical definitions given above see, for example, [42,43].

In this Part I of the paper, we shall be considering problems which are best analysed within the context of cylindrical coordinates, we list the kinematical relations between strains and displacements in such a coordinate system (see, for example, [44]), where the displacement field has components u_r, u_θ and u_z, and from (2.5) we obtain:

$$\varepsilon_{rr} = \frac{\partial u_r}{\partial r}, \quad \varepsilon_{\theta\theta} = \frac{1}{r}\frac{\partial u_\theta}{\partial \theta} + \frac{u_r}{r}, \quad \varepsilon_{zz} = \frac{\partial u_z}{\partial z}, \tag{3}$$

$$\varepsilon_{r\theta} = \frac{1}{2}\left(\frac{1}{r}\frac{\partial u_r}{\partial \theta} + \frac{\partial u_\theta}{\partial r} - \frac{u_\theta}{r}\right), \quad \varepsilon_{rz} = \frac{1}{2}\left(\frac{\partial u_r}{\partial z} + \frac{\partial u_z}{\partial r}\right), \quad \varepsilon_{\theta z} = \frac{1}{2}\left(\frac{\partial u_\theta}{\partial z} + \frac{1}{r}\frac{\partial u_z}{\partial \theta}\right). \tag{4}$$

2.2 Equilibrium equations

If we neglect the effect of body forces and if we consider quasi-static problems, the equation of motion reduces to:

$$\operatorname{div} \mathbf{T} = \mathbf{0}. \tag{5}$$

In the case of cylindrical coordinates (5) reads [44]:

$$\frac{\partial T_{rr}}{\partial r} + \frac{1}{r}\frac{\partial T_{r\theta}}{\partial \theta} + \frac{\partial T_{rz}}{\partial z} + \frac{1}{r}(T_{rr} - T_{\theta\theta}) = 0, \tag{6}$$

$$\frac{\partial T_{r\theta}}{\partial r} + \frac{1}{r}\frac{\partial T_{\theta\theta}}{\partial \theta} + \frac{\partial T_{\theta z}}{\partial z} + \frac{2}{r}T_{r\theta} = 0, \tag{7}$$

$$\frac{\partial T_{rz}}{\partial r} + \frac{1}{r}\frac{\partial T_{\theta z}}{\partial \theta} + \frac{\partial T_{zz}}{\partial z} + \frac{1}{r}T_{rz} = 0. \tag{8}$$

2.3 Constitutive relations

In this work, we consider a nonlinear relation between the linearized strain tensor and the Cauchy stress tensor, which stems from a potential W of the form [7,31,32]:

$$\boldsymbol{\varepsilon} = \frac{\partial W}{\partial \mathbf{T}}, \tag{9}$$

which is a special case of $\boldsymbol{\varepsilon} = \mathfrak{f}(\mathbf{T})$, where we have assumed the existence of a scalar function $W = W(\mathbf{T})$ such that $\mathfrak{f}(\mathbf{T}) = \frac{\partial W}{\partial \mathbf{T}}$. The relation $\boldsymbol{\varepsilon} = \mathfrak{f}(\mathbf{T})$ can be obtained as a special case of a more general class of constitutive relations of the form[4] $\mathfrak{F}(\mathbf{T}, \mathbf{B}) = \mathbf{0}$, which has been proposed by Rajagopal and co-workers [6,15,21,22].

We consider a body[5] wherein $W = W(I_1, I_2, I_3)$, where

$$I_1 = \operatorname{tr} \mathbf{T}, \quad I_2 = \frac{1}{2}\operatorname{tr} \mathbf{T}^2, \quad I_3 = \frac{1}{3}\operatorname{tr} \mathbf{T}^3, \tag{10}$$

[4] Such models can be considered as counterparts of Green elastic solids. In general, the potential can depend on both the stress and the strain. The relation $\boldsymbol{\varepsilon} = \mathfrak{f}(\mathbf{T})$ can be obtained as a special case of $\mathfrak{F}(\mathbf{T}, \mathbf{B}) = \mathbf{0}$ considering the approximation $\mathbf{B} \approx 2\boldsymbol{\varepsilon} + \mathbf{I}$, which is valid when $|\nabla_{\mathbf{X}}\mathbf{u}| \sim O(\delta)$, $\delta \ll 1$. For more details, see, for example, §2.2 of [32].

[5] The notion of material symmetry has only been considered recently, and it has not been studied within the context of the potential depending on both the stress and the deformation gradient [45].

Table 1 Values for the constants used in (13), (14).

α	β 1/Pa	γ 1/Pa	ι 1/Pa^2	E Pa	ν
0.01	9.27681×10^{-8}	4.01995×10^{-9}	10^{-14}	323387085	0.3

and in such a case (9) becomes

$$\boldsymbol{\varepsilon} = W_1\mathbf{I} + W_2\mathbf{T} + W_3\mathbf{T}^2 \tag{11}$$

where we have defined $W_i = \frac{\partial W}{\partial I_i}$, $i = 1, 2, 3$.

Let us consider the following particular expression for W:

$$W(I_1, I_2) = -\frac{\alpha}{\beta}\ln[\cosh(\beta I_1)] + \frac{\gamma}{\iota}\sqrt{1 + 2\iota I_2} \tag{12}$$

where α, β, γ and ι are constant. The exact physical meaning of that particular expression for W will be discussed later on. From (11), (12), we obtain

$$\boldsymbol{\varepsilon} = -\alpha\tanh(\beta I_1)\mathbf{I} + \frac{\gamma}{\sqrt{1 + 2\iota I_2}}\mathbf{T}. \tag{13}$$

We will compare the results obtained for some boundary value problems within the context of (13), with the case of the classical constitutive equation for isotropic linearized elastic bodies:

$$\boldsymbol{\varepsilon} = -\frac{\nu}{E}I_1\mathbf{I} + \frac{(\nu + 1)}{E}\mathbf{T}, \tag{14}$$

where E is Young's modulus and ν is Poisson's ratio.

In order to be able to compare the results, some relationships between the constants α, β, γ and ι and E, ν need to be established; to do so, consider the linearization of (9) (in index notation and with regard to Cartesian coordinates)

$$\varepsilon_{ij} \approx \frac{\partial W}{\partial T_{ij}}(\mathbf{0}) + \frac{\partial^2 W}{\partial T_{ij}\partial T_{kl}}(\mathbf{0})T_{kl}, \tag{15}$$

which in the case of the particular expression for W given in (12), after some simple calculations, leads to

$$\boldsymbol{\varepsilon} \approx -\alpha\beta I_1\mathbf{I} + \gamma\mathbf{T}. \tag{16}$$

Therefore, from (14), we obtain the relations

$$\frac{\nu}{E} = \alpha\beta, \quad \frac{1}{E} = \gamma - \alpha\beta. \tag{17}$$

Let us study the behaviour of a cylinder under the influence of the uniform stress distribution $\mathbf{T} = \sigma_z\mathbf{e}_z \otimes \mathbf{e}_z$, where σ_z is constant. We assume that stress distribution causes a uniform strain distribution of the form $\boldsymbol{\varepsilon} = \varepsilon_{rr}\mathbf{e}_r \otimes \mathbf{e}_r + \varepsilon_{\theta\theta}\mathbf{e}_\theta \otimes \mathbf{e}_\theta + \varepsilon_{zz}\mathbf{e}_z \otimes \mathbf{e}_z$, where ε_{rr}, $\varepsilon_{\theta\theta}$ and ε_{zz} are assumed to be constant. Using such distributions for the stresses and strains, from (13), we have

$$\varepsilon_{zz} = -\alpha\tanh(\beta\sigma_z) + \frac{\gamma}{\sqrt{1 + \iota\sigma_z^2}}\sigma_z, \quad \varepsilon_{rr} = \varepsilon_{\theta\theta} = -\alpha\tanh(\beta\sigma_z). \tag{18}$$

We use the values for the constants that appear in (13) as presented in Table 1; the values for E and ν that are obtained from (17) are presented in the same table.

We must remark that the constitutive theory presented here has been developed very recently and that we have not proposed (13) based on real experimental data. Experimental results pertaining to the relationship between the linearized strain and the stress being nonlinear can be found, for example, in the experimental papers [1–3,9,10] and the references cited therein. However, these experiments present one-dimensional data, and as infinity of three-dimensional models can lead to the same one-dimensional representation, it is impossible to decide the appropriate three-dimensional model on the basis of such experiments (see Karra and Rajagopal [46]).

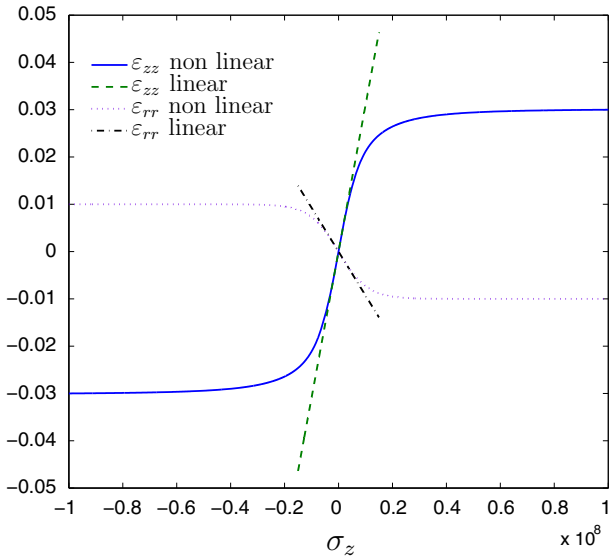

Fig. 1 Results for $\varepsilon_{zz}(\sigma_z)$ and $\varepsilon_{rr}(\sigma_z)$ for a cylinder under the effect of the uniform axial stress distribution $\mathbf{T} = \sigma_z \mathbf{e}_z \otimes \mathbf{e}_z$. Comparison of the predictions of the nonlinear model (13), and the linearized Eq. (14). Axial stress σ_z in (Pa)

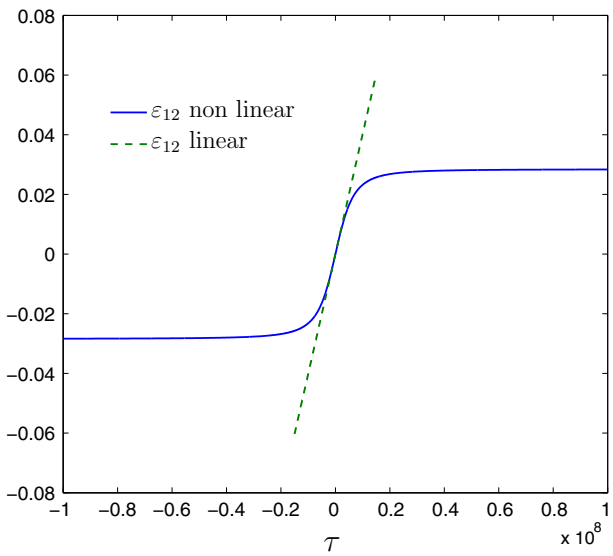

Fig. 2 Results for $\varepsilon_{12}(\tau)$ for a slab under the effect of the uniform shear stress distribution $\mathbf{T} = \tau(\mathbf{e}_1 \otimes \mathbf{e}_2 + \mathbf{e}_2 \otimes \mathbf{e}_1)$. Comparison of the predictions of the nonlinear model (13), and the linearized Eq. (14). The shear stress τ is in (Pa)

In Fig. 1 we portray the variations of $\varepsilon_{zz}(\sigma_z)$ and $\varepsilon_{rr}(\sigma_z)$ that correspond to the two constitutive relations (13), (14) and the values of the constants presented in Table 1. We see that the use of (13) implies a strain-limiting behaviour for the axial and also for the radial components of the strain. Using (17), the linearized constitutive equation (14) gives approximately the same result as the nonlinear model for 'small' stresses; also the nonlinear model and the linear model agree, when the strains are below 1 %, but diverge for strains larger than 1 %.

Let us consider a slab, defined in Cartesian coordinates, in the undeformed configuration defined by $-L_1 \leq x_1 \leq L_1$, $L_2 \leq x_2 \leq L_2$, $L_2 \leq x_3 \leq L_3$, under the effect of the uniform stress distribution $\mathbf{T} = \tau(\mathbf{e}_1 \otimes \mathbf{e}_2 + \mathbf{e}_2 \otimes \mathbf{e}_1)$. Let us further suppose that the body is defined by the constitutive relations (13) or (14), with the material constants as given in Table 1. The behaviour for $\varepsilon_{12}(\tau)$ is depicted in Fig. 2, where again we observe a strain limiting behaviour if we use (13), and as in the earlier case the results for the linearized body and the nonlinear model are similar when the shear stress τ is 'small'.

Table 2 Cases to be considered for the tube under axial shear and pressure applied on the inner surface.

Outer radius $r_{\mathbf{o}}$ (m)	Inner radial normal stress P_{i} (Pa)	C_0 (N/m)
Case A		
0.11	10^9	-2×10^8
0.2	2×10^9	-2×10^8
10	2×10^7	-10^6
Case B		
0.11	7×10^7	-2×10^8
0.2	6×10^8	-2×10^8
10	2×10^7	-10^6

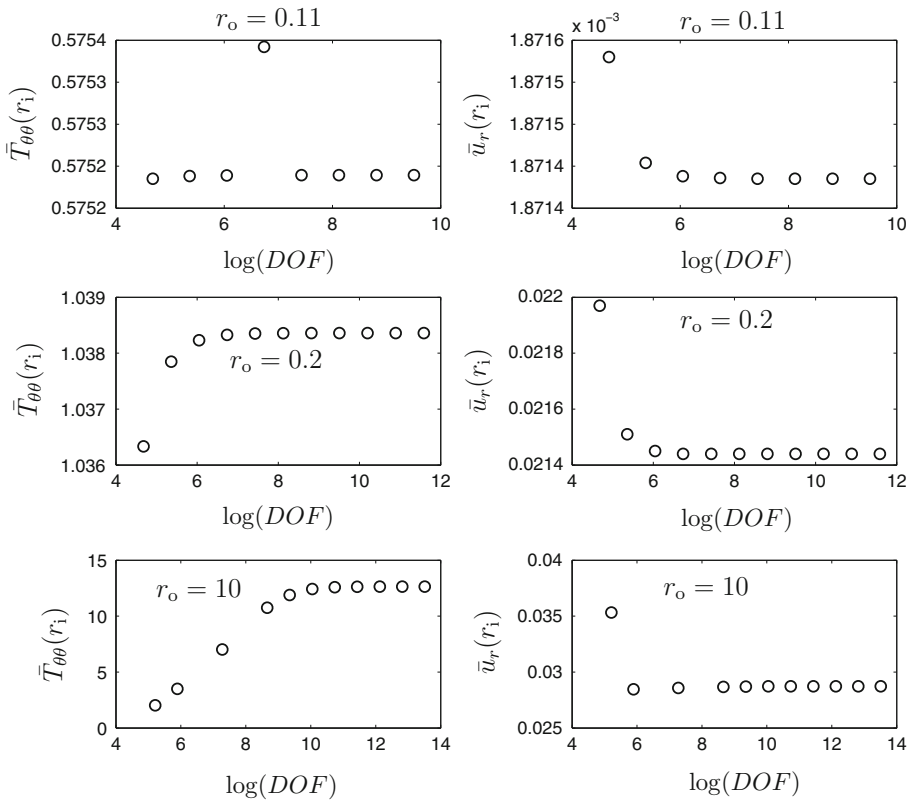

Fig. 3 Influence of the mesh density for the three examples of tubes presented in Table 2, which are under the effect of an axial shear and an inner radial normal stress. Dimensionless azimuthal stress $\bar{T}_{\theta\theta} = \frac{T_{\theta\theta}}{P_{\mathrm{i}}}$ and dimensionless radial displacement $\bar{u}_r = \frac{u_r}{r_{\mathrm{i}}}$ evaluated at $r = r_{\mathrm{i}}$, vs the natural logarithm of the degrees of freedom *DOF*

2.4 Summary of the boundary value problems

In Sects. 3 and 4, we study some boundary value problems, within the context of nonhomogeneous distributions of stresses, generating nonhomogeneous distributions for the displacement field and strains, using the new class of constitutive relation (13). We compare the results that we obtain with the results for the classical constitutive equation for isotropic linearized elastic bodies (14), for different values of the material constants provided in Table 1. We solve the boundary value problems using (9) in the following manner:

- We appeal to the semi-inverse methodology and assume a simplified expression for the stress tensor $\mathbf{T}$, which satisfies the equilibrium equation (5) (ignoring the body force field):

$$\operatorname{div} \mathbf{T} = \mathbf{0}.$$

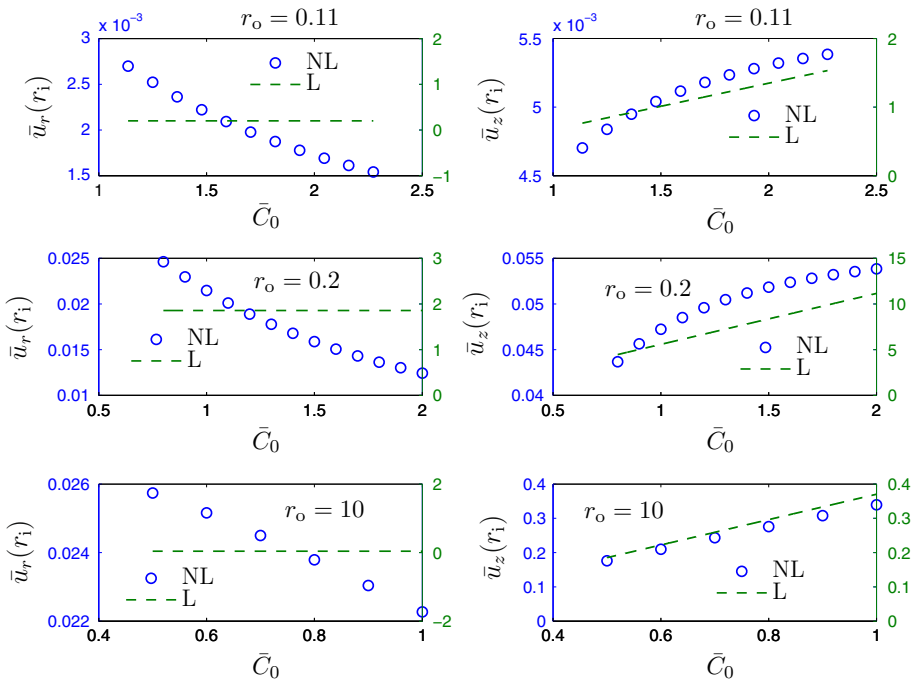

Fig. 4 Tube under axial shear and inner radial normal stress. Influence of the parameter $\bar{C}_0$ on the dimensionless radial displacement $\bar{u}_r = \frac{u_r}{r_i}$, and the dimensionless axial component of the displacement $\bar{u}_z = \frac{u_z}{r_i}$, which are evaluated at $r = r_i$. A comparison is presented between the results obtained considering a linearized elastic body (L) [Eq. (14), the scale for each plot is on the *right*], and the nonlinear model (NL) [see Eq. (13), the scale for the each plot is on the *left*]. The radii $r_o = 0.11$; 0.2; 10 m indicate the three different tubes considered (see Table 2). The parameter $\bar{C}_0$ is negative

- Using the kinematic relation (2) and the above stress tensor, we solve the equation

$$\frac{1}{2}(\nabla \mathbf{u} + \nabla \mathbf{u}^{\mathrm{T}}) = \frac{\partial W}{\partial \mathbf{T}}.$$

  The equations are solved to find simultaneously the components of the stress tensor and the displacement field, as illustrated in Sects. 3 and 4. It is worth observing that when the unknowns are the stress and the displacement field, the compatibility of strains is a non-issue (see Rajagopal and Srinivasa [47]).
- For the above problem, we consider 'directly' the usual boundary conditions $\mathbf{u} = \hat{\mathbf{u}}$, which is known on $\partial\kappa_r(\mathcal{B})_u$, and $\mathbf{Tn} = \hat{\mathbf{t}}$, where $\mathbf{t}$ is an external traction on $\partial\kappa_r(\mathcal{B})_t$, where $\partial\kappa_r(\mathcal{B})_u \cup \partial\kappa_r(\mathcal{B})_t = \partial\kappa_r(\mathcal{B})$ and $\partial\kappa_r(\mathcal{B})_u \cap \partial\kappa_r(\mathcal{B})_t = \emptyset$.

3 A tube under telescopic shear and inflation

In this problem, we study the behaviour of a tube defined by $r_i \le r \le r_o$, $0 \le \theta \le 2\pi$, $0 \le z \le L$ under the effect of the stress distribution $\mathbf{T} = \mathbf{T}(r)$, which we assume is caused by an internal pressure and the application of a surface shear. If $T_{ij} = T_{ij}(r)$ the equilibrium equations (6)–(8) are satisfied if:

$$T_{\theta\theta} = r\frac{\mathrm{d}T_{rr}}{\mathrm{d}r} + T_{rr}, \quad T_{r\theta} = \frac{C_1}{r^2}, \quad T_{rz} = \frac{C_0}{r}, \tag{19.1–3}$$

where C_1, C_0 are constants. For simplicity, in this section, we assume that $C_1 = 0$. We further assume now that the stress distribution is of the form:

$$\mathbf{T} = T_{rr}(r)\mathbf{e}_r \otimes \mathbf{e}_r + T_{\theta\theta}(r)\mathbf{e}_\theta \otimes \mathbf{e}_\theta + T_{zz}(r)\mathbf{e}_z \otimes \mathbf{e}_z + \frac{C_0}{r}\mathbf{e}_r \otimes \mathbf{e}_z, \tag{20}$$

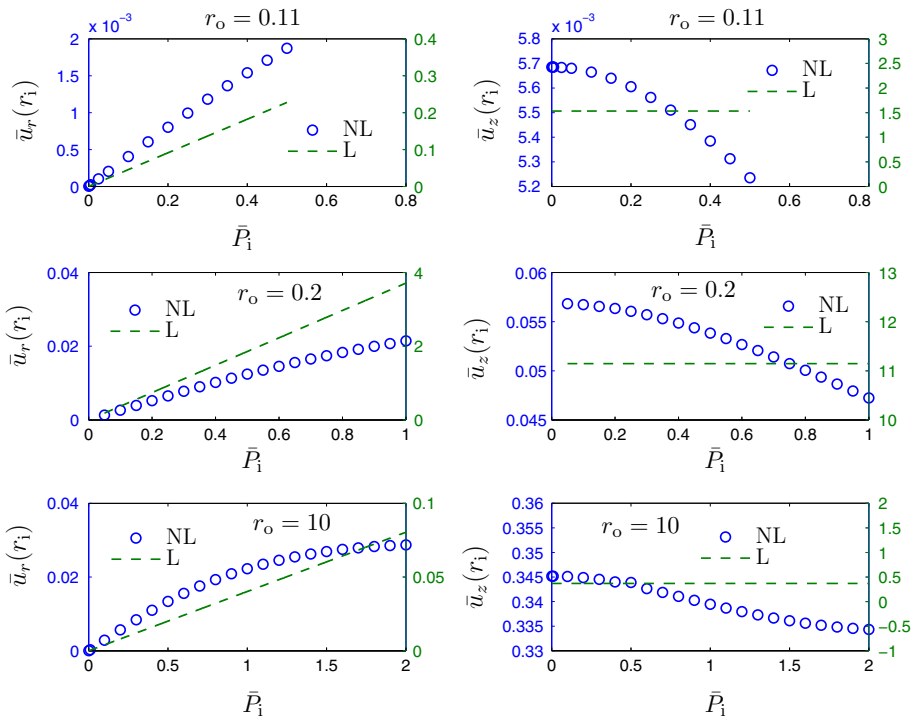

Fig. 5 Tube under axial shear and inner radial normal stress. Influence of the inner radial normal stress P_i on the dimensionless radial displacement $\bar{u}_r = \frac{u_r}{r_i}$, and the dimensionless axial component of the displacement $\bar{u}_z = \frac{u_z}{r_i}$, which are evaluated at $r = r_i$. A comparison is presented between the results obtained considering a linearized elastic body (L) [Eq. (14)] and the nonlinear model (NL) [see Eq. (13)]. The radii $r_o = 0.11; 0.2; 10$ m indicate the three different tubes considered (see Table 2). The influence of P_i is studied indirectly considering the dimensionless radial normal stress $\bar{P}_i = \frac{r_i P_i}{C_0}$.

which produces a the displacement field of the form[6]

$$\mathbf{u} = u_r(r)\mathbf{e}_r + u_z(r)\mathbf{e}_z. \tag{21}$$

From (3), (4), we observe that the nonzero components of the linearized strain tensor are:

$$\varepsilon_{rr} = \frac{\mathrm{d}u_r}{\mathrm{d}r}, \quad \varepsilon_{\theta\theta} = \frac{u_r}{r}, \quad \varepsilon_{rz} = \frac{1}{2}\frac{\mathrm{d}u_z}{\mathrm{d}r}. \tag{22}$$

Substituting (20) and (22) in (11) we obtain:

$$\frac{\mathrm{d}u_r}{\mathrm{d}r} = W_1 + W_2 T_{rr} + W_3\left(T_{rr}^2 + \frac{C_0^2}{r^2}\right), \tag{23}$$

$$\frac{u_r}{r} = W_1 + W_2\left(r\frac{\mathrm{d}T_{rr}}{\mathrm{d}r} + T_{rr}\right) + W_3\left(r\frac{\mathrm{d}T_{rr}}{\mathrm{d}r} + T_{rr}\right)^2, \tag{24}$$

$$0 = W_1 + W_2 T_{zz} + W_3\left(T_{zz}^2 + \frac{C_0^2}{r^2}\right), \tag{25}$$

$$\frac{1}{2}\frac{\mathrm{d}u_z}{\mathrm{d}r} = W_2\frac{C_0}{r} + W_3\frac{C_0}{r}(T_{rr} + T_{zz}). \tag{26}$$

We need to solve (23)–(26) to find $T_{rr}(r)$, $T_{zz}(r)$, $u_r(r)$ and $u_z(r)$. In particular, Eq. (25) could be used in order to find T_{zz}.

[6] It is possible that the choices made for the stress field and the displacement field might not be compatible. Also, even if a solution of the form sought exists, it is possible that the problem under consideration might have solutions other than that sought as the problem is nonlinear.

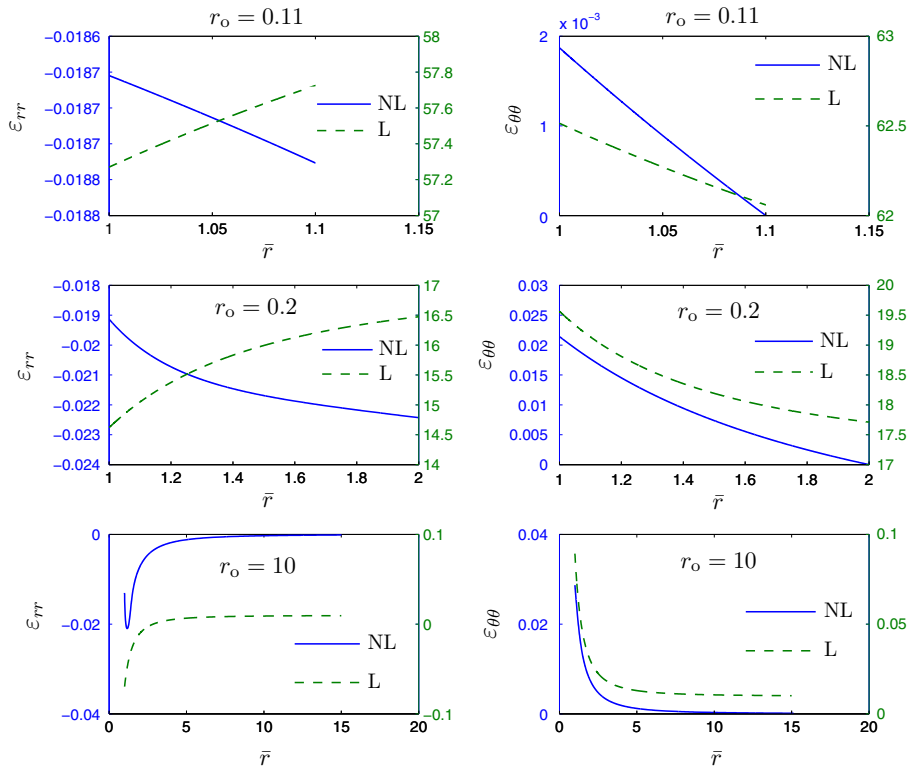

Fig. 6 Tube under axial shear and inner radial normal stress. Results for the radial and azimuthal components of the strain using the boundary conditions defined as Case (A) [see (27) and Table 2], considering the constitutive equations (14) for linearized elastic bodies (L), and the nonlinear model (13) (NL), versus the dimensionless radius $\bar{r} = \frac{r}{r_i}$. The radii $r_o = 0.11; 0.2; 10$ m indicate the three different tubes considered in Table 2. For the tube $r_o = 10$ m results are presented for a limited range of $\bar{r}$.

Regarding the boundary conditions we consider two cases:

$$\text{(A)}: \quad T_{rr}(r_i) = -P_i, \quad u_r(r_o) = 0, \quad u_z(r_o) = 0, \tag{27}$$

$$\text{(B)}: \quad T_{rr}(r_i) = -P_i, \quad T_{rr}(r_o) = 0, \quad u_z(r_o) = 0. \tag{28}$$

In the first case, we assume that the inner surface of the tube is under the effect of a normal stress P_i, while the radial and axial components of the displacement are constrained on the outer surface of the tube. In the second case, we assume the same normal stress is applied on the inner surface, while on the outer surface, there is no external radial traction. In both cases, we have the effect of an external normal stress, and besides that load we need to consider the influence of C_0. If $C_0 \leq 0$, then C_0/r_i corresponds to an axial external applied shear on the inner surface of the tube.

Now, we obtain solutions to (23)–(26), in the case we have a linearized elastic body (14), and also in the case of the new constitutive relation (13). For linearized elastic bodies (14), Eqs. (23)–(26) can be solved exactly and in Case (A) [see (27)] we have (see Chapter XIV of [48]):

$$T_{rr} = -\frac{P_i r_i^2[r^2 + r_o^2(1-2\nu)]}{r^2[r_i^2 + r_o^2(1-2\nu)]}, \quad T_{\theta\theta} = -\frac{P_i r_i^2[r^2 + r_o^2(2\nu-1)]}{r^2[r_i^2 + r_o^2(1-2\nu)]}, \tag{29}$$

$$T_{zz} = -\frac{2P_i r_i^2 \nu}{[r_i^2 + r_o^2(1-2\nu)]}, \tag{30}$$

$$u_r = \frac{P_i r_i^2(r^2 - r_o^2)(2\nu^2 + \nu - 1)}{Er[r_i^2 + r_o^2(1-2\nu)]}, \quad u_z = \frac{2C_0(1+\nu)}{E}\log\left(\frac{r}{r_o}\right), \tag{31.1,2}$$

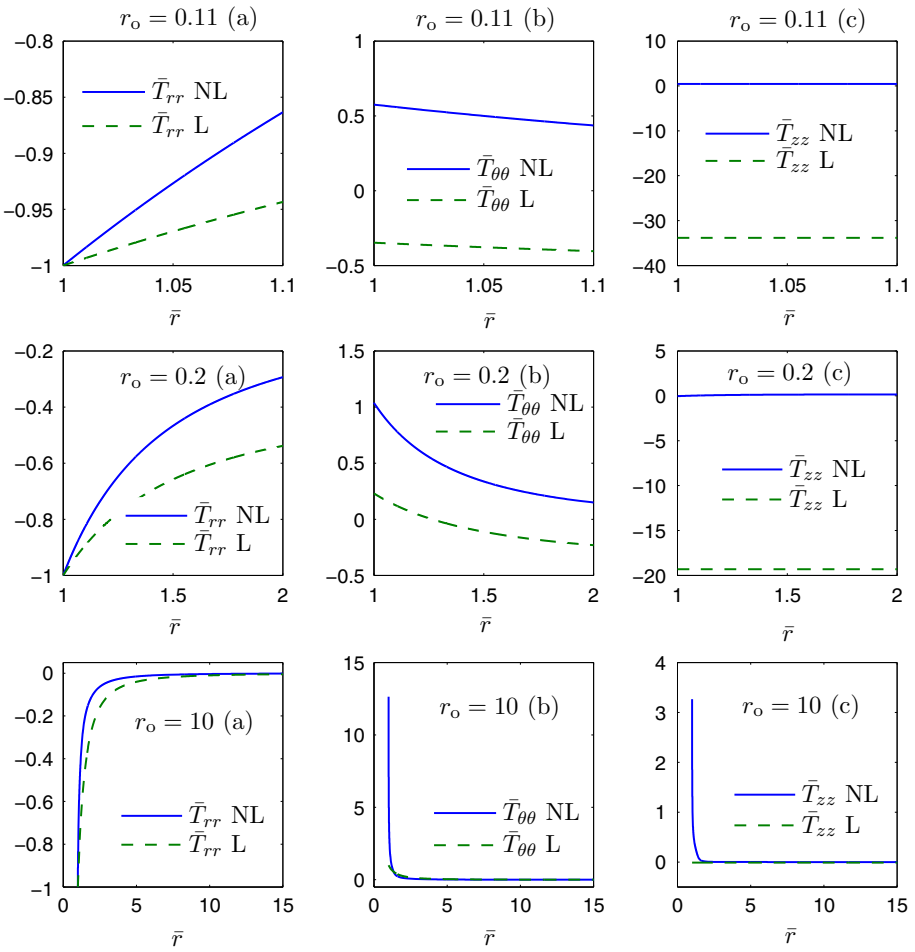

Fig. 7 Tube under the influence of axial shear and inner radial normal stress [in the case of boundary conditions defined as Case (A); see (27) and Table 2]. Results for the dimensionless radial, azimuthal and axial components of the stress tensor $\bar{T}_{rr} = \frac{T_{rr}}{P_i}$, $\bar{T}_{\theta\theta} = \frac{T_{\theta\theta}}{P_i}$ and $\bar{T}_{zz} = \frac{T_{zz}}{P_i}$, respectively, as functions of the dimensionless radius $\bar{r} = \frac{r}{r_i}$. The radii $r_o = 0.11; 0.2; 10$ m indicate the three different tubes considered (see Table 2). For each figure results are presented for a linearized elastic body (14) (L), and the new class of constitutive relations (13) (NL). For the tube with $r_o = 10$ m results are presented for a limited range of $\bar{r}$

while in Case (B) [see (28)] we obtain:

$$T_{rr} = \frac{Pr_i^2(r_o^2 - r^2)}{r^2(r_i^2 - r_o^2)}, \quad T_{\theta\theta} = -\frac{Pr_i^2(r_o^2 + r^2)}{r^2(r_i^2 - r_o^2)}, \quad T_{zz} = -\frac{2P_i r_i^2 \nu}{(r_i^2 - r_o^2)}, \tag{32}$$

$$u_r = \frac{Pr_i^2(1+\nu)[r^2(2\nu - 1) - r_o^2]}{Er(r_i^2 - r_o^2)}, \tag{33}$$

and the expression for $u_z(r)$ is the same as in (31.2).

When the constitutive relation (13) is used, we solve (23)–(26) using a numerical method. We use the finite element method, for which we need to manipulate (23)–(26). Equations (23), (24) can be reduced to the following nonlinear second-order differential equation for $T_{rr}(r)$:

$$\frac{\mathrm{d}}{\mathrm{d}r}\left\{r\left[W_1 + W_2\left(r\frac{\mathrm{d}T_{rr}}{\mathrm{d}r} + T_{rr}\right) + W_3\left(r\frac{\mathrm{d}T_{rr}}{\mathrm{d}r} + T_{rr}\right)^2\right]\right\} = W_1 + W_2 T_{rr} + W_3\left(T_{rr}^2 + \frac{C_0^2}{r^2}\right), \tag{34}$$

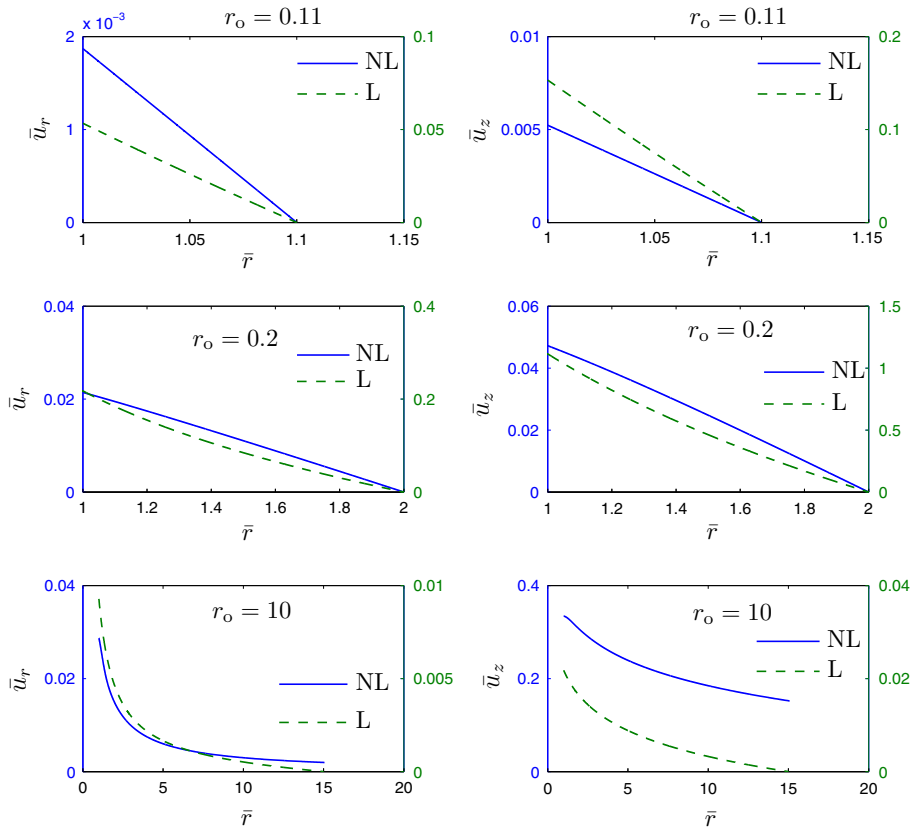

Fig. 8 Tube under the influence of axial shear and radial normal stress applied on $r = r_i$ [for the boundary conditions indicated as Case (A); see (27) and Table 2]. Results are presented for the dimensionless radial and axial components of the displacement vector $\bar{u}_r = \frac{u_r}{r_i}$, $\bar{u}_z = \frac{u_z}{r_i}$, as functions of the dimensionless radius $\bar{r} = \frac{r}{r_i}$. The radii $r_o = 0.11; 0.2; 10$ m indicate the three different tubes considered. For each figure results are presented for a linearized elastic body (14) (L), and the new class of constitutive relations (13) (NL). For the tube with $r_o = 10$ m results are presented for a limited range of $\bar{r}$

which, if we define $\Gamma = r\left[W_1 + W_2\left(r\frac{\mathrm{d}T_{rr}}{\mathrm{d}r} + T_{rr}\right) + W_3\left(r\frac{\mathrm{d}T_{rr}}{\mathrm{d}r} + T_{rr}\right)^2\right]$ and $F = W_1 + W_2 T_{rr} + W_3\left(T_{rr}^2 + \frac{C_0^2}{r^2}\right)$, can be written as

$$\frac{\mathrm{d}\Gamma}{\mathrm{d}r} = F, \tag{35}$$

which can be solved with a standard nonlinear finite element code. Regarding Eq. (25), which could be used to find, for example, $T_{zz}(r)$, a solution is found by solving the second- order differential equation

$$\frac{\mathrm{d}}{\mathrm{d}r}\left\{W_1 + W_2\frac{\mathrm{d}h}{\mathrm{d}r} + W_3\left[\left(\frac{\mathrm{d}h}{\mathrm{d}r}\right)^2 + \frac{C_0^2}{r^2}\right]\right\} = 0, \tag{36}$$

where we have defined $T_{zz} = \frac{\mathrm{d}h}{\mathrm{d}r}$. Finally, regarding (26), if we define $u_z(r) = \frac{\mathrm{d}g}{\mathrm{d}r}$, we obtain

$$\frac{\mathrm{d}^2 g}{\mathrm{d}r^2} = W_2\frac{C_0}{r} + W_3\frac{C_0}{r}\left(T_{rr} + \frac{\mathrm{d}h}{\mathrm{d}z}\right). \tag{37}$$

The three nonlinear coupled second-order differential equations (34), (36) and (37) are solved using the finite element method in order to find $T_{rr}(r)$, $h(r)$ and $g(r)$. Regarding the boundary conditions, from (27) for Case (A) we have the conditions:

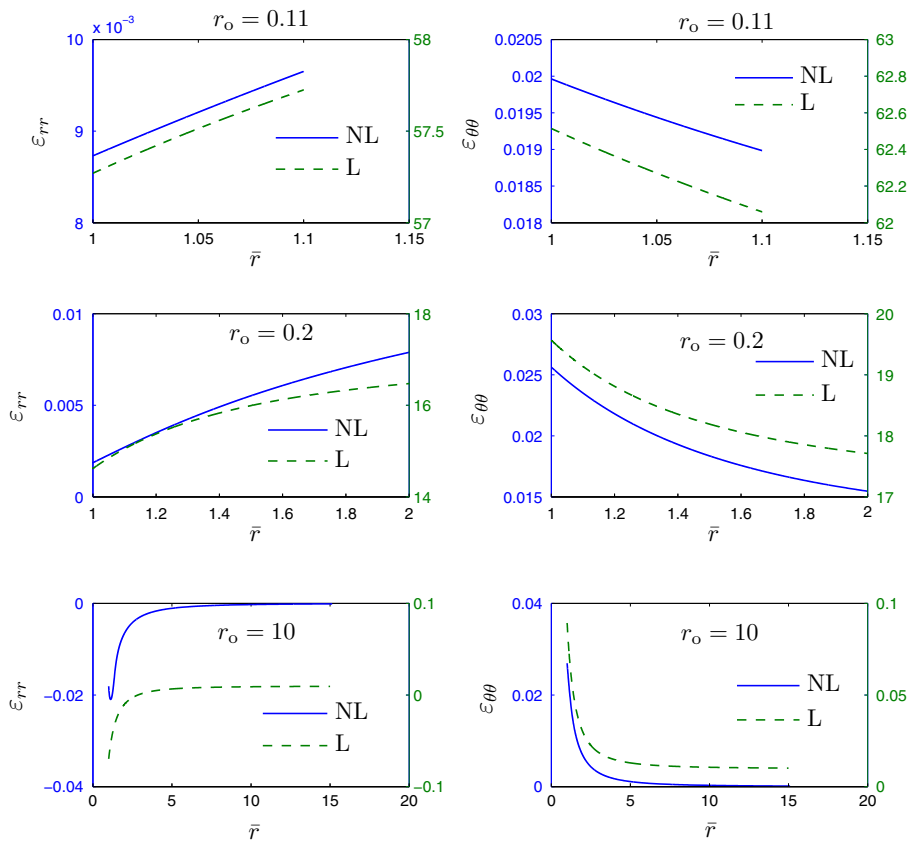

Fig. 9 Tube under the effect of axial shear and radial normal stress applied on the surface $r = r_i$. Results for the radial and azimuthal components of the strain, for the boundary conditions indicated as Case (B) [see (28) and Table 2], for the constitutive equation (14) for linearized elastic bodies (L), and the nonlinear model (13) (NL), versus the dimensionless radius $\bar{r} = \frac{r}{r_i}$. The radii $r_o = 0.11; 0.2; 10$ m indicate the three different tubes considered. For the tube with $r_o = 10$ m results are presented for a limited range of $\bar{r}$

$$T_{rr}(r_i) = -P_i, \quad \left\{ r \left[W_1 + W_2 \left(r \frac{dT_{rr}}{dr} + T_{rr} \right) + W_3 \left(r \frac{dT_{rr}}{dr} + T_{rr} \right)^2 \right] \right\}_{r=r_o} = 0, \qquad (38.1,2)$$

$$h(r_i) = 0, \quad \left\{ W_1 + W_2 \frac{dh}{dr} + W_3 \left[\left(\frac{dh}{dr} \right)^2 + \frac{C_0^2}{r^2} \right] \right\}_{r=r_o} = 0, \qquad (39)$$

$$g(r_i) = 0, \quad \left. \frac{dg}{dr} \right|_{r=r_o} = 0. \qquad (40)$$

When considering (28) for Case (B) condition (38.2) changes to $T_{rr}(r_o) = 0$ and the rest of the conditions remains the same.

Three examples are considered for the tube, where the external radii are different, but the internal radius $r_i = 0.1$ m is kept the same. These three cases are presented in Table 2.

For each case, we list the maximum radial normal stress and value of C_0 that we were able to use without having problems with regard to the convergence of the numerical scheme. Equations (35)–(37) are solved using the programme Comsol 4.2 [49].

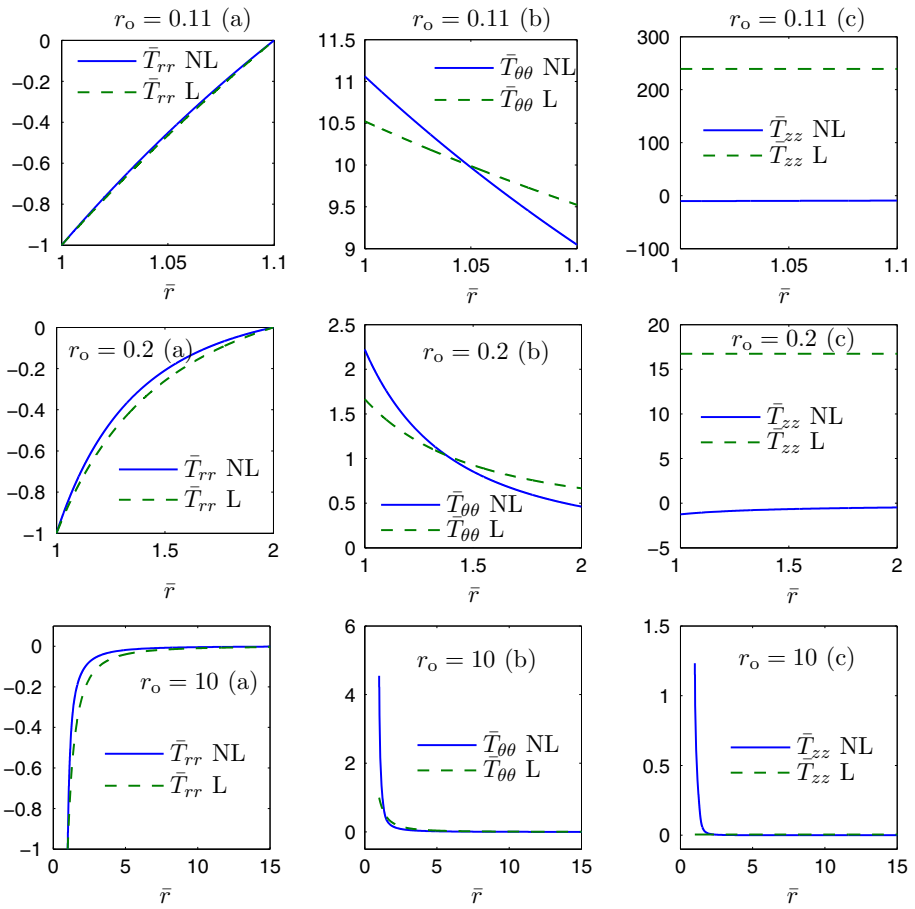

Fig. 10 Tube under the effect of axial shear and radial normal stress applied on the surface $r = r_i$. Results for the dimensionless radial, azimuthal and axial components of the stress tensor $\bar{T}_{rr} = \frac{T_{rr}}{P_i}$, $\bar{T}_{\theta\theta} = \frac{T_{\theta\theta}}{P_i}$ and $\bar{T}_{zz} = \frac{T_{zz}}{P_i}$, respectively, as functions of the dimensionless radius $\bar{r} = \frac{r}{r_i}$. Results are obtained for the boundary conditions defined as Case (B) [see (28) and Table 2], for the constitutive equation (14) for linearized elastic bodies (L), and the nonlinear model (13) (NL). The radii $r_o = 0.11; 0.2; 10$ m indicate the three different tubes considered. For the tube with $r_o = 10$ m results are presented for a limited range of $\bar{r}$

In the different plots to be presented in this section, we consider the following dimensionless quantities:

$$\bar{r} = \frac{r}{r_i}, \quad \bar{T}_{rr} = \frac{T_{rr}}{P_i}, \quad \bar{T}_{\theta\theta} = \frac{T_{\theta\theta}}{P_i}, \quad \bar{T}_{zz} = \frac{T_{zz}}{P_i} \quad \bar{u}_r = \frac{u_r}{r_i}, \quad \bar{u}_z = \frac{u_z}{r_i}, \tag{41.1–6}$$

$$\bar{C}_0 = \frac{C_0}{r_i P_i}, \quad \bar{P}_i = \frac{1}{\bar{C}_0}. \tag{42}$$

In order to evaluate the influence of the mesh density when solving (35)–(37) using the finite element method, in Fig. 3 we present results for the azimuthal component of the stress and the radial displacement for the tube [in the case of the nonlinear model (13)], which are evaluated at $r = r_i$ for the three tubes presented in Table 2 as (Case A), versus the natural logarithm of the degrees of freedom.

In Fig. 4, we depict the behaviour of $\bar{u}_r(r_i)$ and $\bar{u}_z(r_i)$ for the three different tubes considered in Table 2 indicated as (Case A), as functions of the constant C_0 (the parameter $\bar{C}_0$). A comparison between the results obtained considering (13) and (14) is presented, where L denotes the use of the linearized constitutive relation (14), and NL denotes the use of the nonlinear model (13). In the case of (14), it is easy to see that there is no influence of C_0 on u_r, and therefore for such plots, we observe that $\bar{u}_r(r_i)$ is constant [see (31.2)].

In Fig. 5, results are presented for $\bar{u}_r(r_i)$ and $\bar{u}_z(r_i)$ for the three different tubes considered in Table 2 (Case A), as functions of the inner pressure P_i (presented indirectly through the dimensionless pressure $\bar{P}_i = \frac{1}{\bar{C}_0}$). In this case, for linearized elastic bodies [denoted L in the figure, see Eq. (14)], we see that $\bar{u}_z(\bar{P}_i)$ is constant.

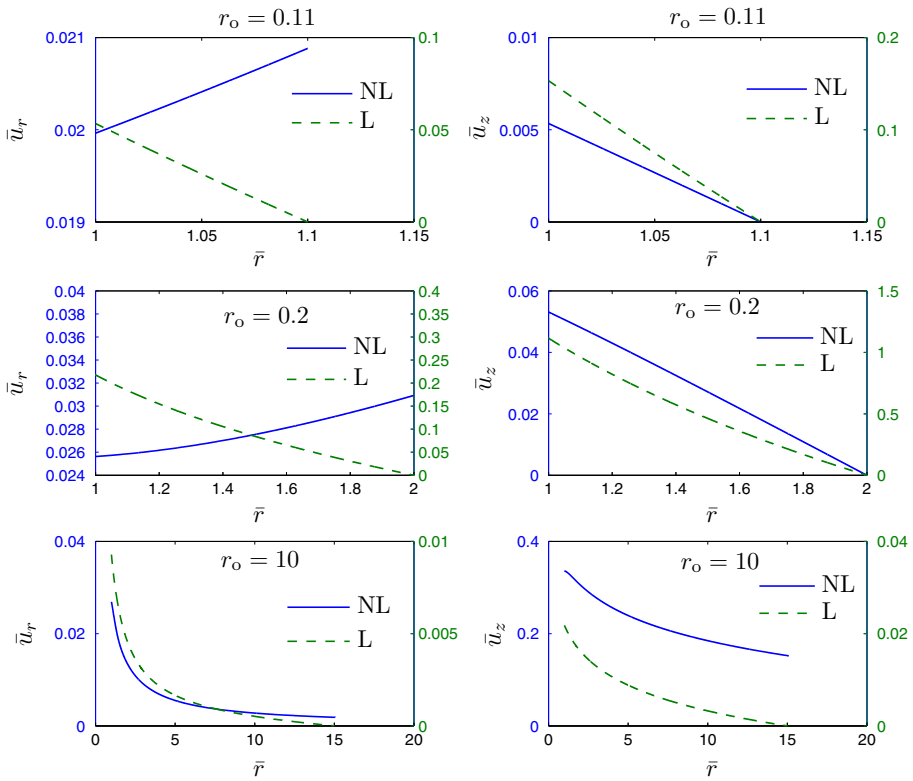

Fig. 11 Tube under the effect of axial shear and normal radial stress applied on the surface $r = r_i$. Results for the dimensionless radial and axial components of the displacement vector $\bar{u}_r = \frac{u_r}{r_i}$, $\bar{u}_z = \frac{u_z}{r_i}$, as functions of the dimensionless radius $\bar{r} = \frac{r}{r_i}$. Results are obtained for the boundary conditions indicated as Case (B) [see (28) and Table 2], for the constitutive equation (14) for linearized elastic bodies (L), and the nonlinear model (13) (NL). The radii $r_o = 0.11; 0.2; 10$ m indicate the three different tubes considered. For the tube with $r_o = 10$ m results are presented for a limited range of $\bar{r}$.

Table 3 Cases to be considered for the tube under circumferential shear and radial normal stress applied on the inner surface

Outer radius r_o (m)	Inner radial normal stress P_i (Pa)	C_0 (N)	λ_z
Case A			
0.11	1.5×10^8	-10^5	1.02
0.2	1.5×10^8	-10^5	1.01
10	10^7	-10^5	1.02
Case B			
0.11	7×10^6	-10^5	1.02
0.2	1.5×10^7	-10^5	1.01
10	10^7	-10^5	1.02

Regarding $\bar{u}_r(\bar{P}_i)$ from (31.1), we see that the behaviour is linear.

In Fig. 6, we portray results for the radial and azimuthal components of the linearized strain tensor, in terms of the dimensionless radius $\bar{r} = \frac{r}{r_i}$, for the three different tubes presented in Table 2, for the linearized constitutive equation (14) (L) and the nonlinear model (13) (NL), corresponding to the boundary conditions Case (A) [see (27) and Table 2]. In the case of the linearized constitutive equations, in particular for the tubes $r_o = 0.11; 0.2$ m (first and second figures from top to bottom in Fig. 6), we notice immediately that the magnitude of such components is well above the limits considered for the linearized theory and the domain wherein the linearized strain tensor is applicable. On the other hand, the results obtained for the nonlinear constitutive relation (13) (NL), the strains remain small, and the maximum value is less than 0.04.

In Fig. 7, we have results for the normal components of the stress tensor, for the boundary conditions indicated as Case (A) [see (27) and Table 2]. The figure corresponding to $r_o = 0.11$(a), $r_o = 0.2$(a) and $r_o = 10$(a) display results for the dimensionless radial component $\bar{T}_{rr} = \frac{T_{rr}}{P_i}$ of the stress tensor for the tubes

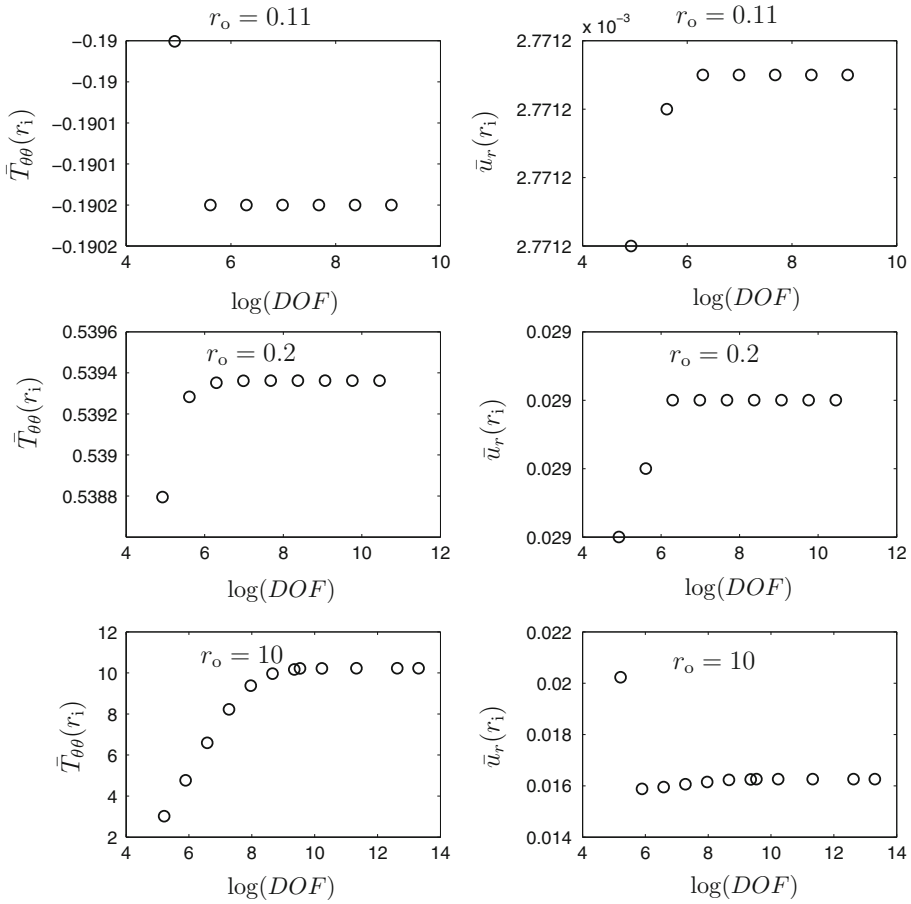

Fig. 12 Influence of the mesh density for the three examples presented in Table 3 for a tube under the influence of circumferential shear, axial extension and inner radial normal stress. Results for the dimensionless stress $\bar{T}_{\theta\theta} = \frac{T_{\theta\theta}}{P_i}$ and the dimensionless radial displacement $\bar{u}_r = \frac{u_r}{r_i}$ (evaluated at $r = r_i$), versus the natural logarithm of the degrees of freedom

with outer radii $r_o = 0.11$; 0.2; 10 m, respectively; while figures corresponding to $r_o = 0.11$(b), $r_o = 0.2$(b) and $r_o = 10$(b) portray results for the dimensionless azimuthal component $\bar{T}_{\theta\theta} = \frac{T_{\theta\theta}}{P_i}$ of the stress tensor; finally, the plots corresponding to $r_o = 0.11$(c), $r_o = 0.2$(c) and $r_o = 10$(c) provide results for the dimensionless axial component $\bar{T}_{zz} = \frac{T_{zz}}{P_i}$ of the stress tensor. From these results, we can see that the largest difference between the results for the linearized elastic body (14) and the new class of elastic bodies (13) manifests itself in the case $r_o = 0.11$ m. A very significant difference can be observed for $\bar{T}_{\theta\theta}$ and $\bar{T}_{zz}$, where in particular we notice that such components of the stress can be very large in the case of the linearized elastic solid thereby violating the basic assumption within which the approximation is derived, while from Fig. 6 we notice that the strains remain small for the new class of constitutive relations (13).

Finally, regarding the boundary conditions indicated as Case (A) [see (27) and Table 2], in Fig. 8 we present results for the dimensionless radial and axial components of the displacement field $\bar{u}_r = \frac{u_r}{r_i}$, $\bar{u}_z = \frac{u_z}{r_i}$, comparing results using the linearized constitutive relation (14) (L), and the new class of elastic bodies (13) (NL).

In Figs. 9, 10 and 11, we find results similar to those presented in Figs. 6, 7 and 8, respectively, for the case of boundary conditions defined as Case (B) [see (28) and Table 2].

4 Circumferential shear and inflation of a tube

We now study the same tube considered in Sect. 3 defined by: $r_i \leq r \leq r_o$, $0 \leq \theta \leq 2\pi$, $0 \leq z \leq L$, subjected to the stress distribution $\mathbf{T} = \mathbf{T}(r)$, which we assume is caused by an internal pressure and a surface

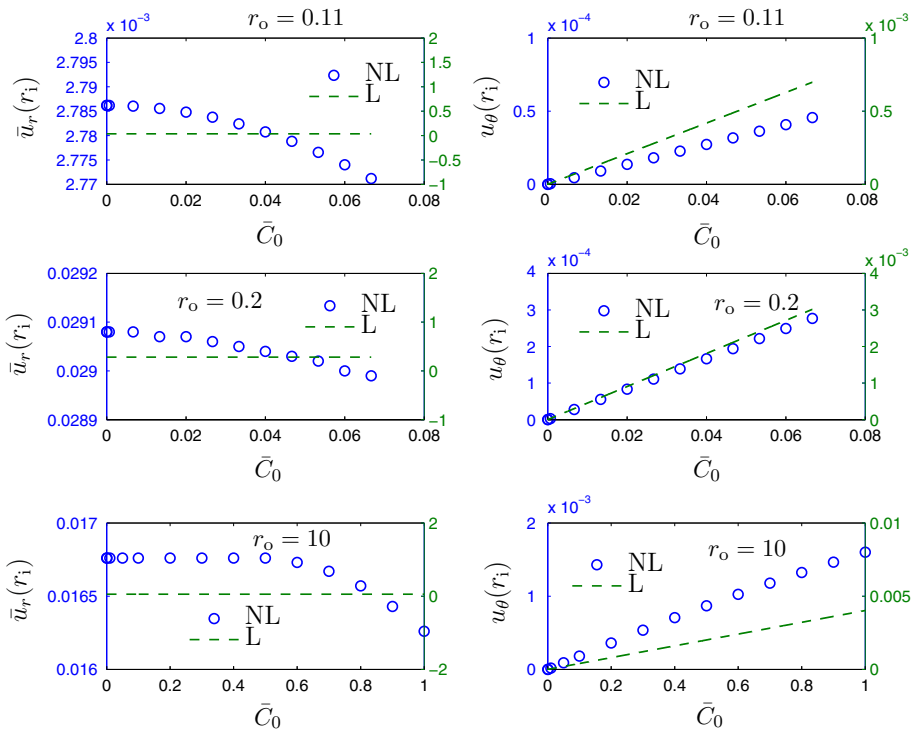

Fig. 13 Tube under the influence of circumferential shear, stretch and radial normal stress applied on the inner surface $r = r_i$. Influence of the parameter $\bar{C}_0$ on the dimensionless radial displacement $\bar{u}_r = \frac{u_r}{r_i}$, and the θ component of the displacement u_θ, which are evaluated at $r = r_i$. A comparison of the results obtained for a linearized elastic body (L) [Eq. (14), see the scale on the right of each plot] and the nonlinear model (NL) [see Eq. (13)] are presented (notice the scale on the left for each plot). The radii $r_o = 0.11$; 0.2; 10 m indicate the three different tubes considered. The parameter $\bar{C}_0$ is negative

shear that is different from that considered previously in Sect. 3. In the earlier section, we had ignored the circumferential shearing and assumed that the tube was only subject to telescopic shearing. In this section, we ignore the telescopic shearing and include circumferential shearing. If $T_{ij} = T_{ij}(r)$ the equilibrium equations (6)–(8) are satisfied if (19) holds. In this section, we assume that $T_{r\theta} = \frac{C_0}{r^2}$ and $T_{rz} = 0$, and we add the effect of an axial stretching of the tube, we therefore have the stress distribution [where $T_{\theta\theta}$ is given by (19.1)]:

$$\mathbf{T} = T_{rr}(r)\mathbf{e}_r \otimes \mathbf{e}_r + T_{\theta\theta}(r)\mathbf{e}_\theta \otimes \mathbf{e}_\theta + T_{zz}(r)\mathbf{e}_z \otimes \mathbf{e}_z + \frac{C_0}{r^2}\mathbf{e}_r \otimes \mathbf{e}_\theta \tag{43}$$

which we assume produces the displacement field

$$\mathbf{u} = u_r(r)\mathbf{e}_r + u_\theta(r)\mathbf{e}_\theta + (\lambda_z - 1)z\mathbf{e}_z, \tag{44}$$

where $\lambda_z > 0$ is a constant. This displacement field leads to the following nonzero components for the strain tensor [see (3)–(4)]:

$$\varepsilon_{rr} = \frac{\mathrm{d}u_r}{\mathrm{d}r}, \quad \varepsilon_{\theta\theta} = \frac{u_r}{r}, \quad \varepsilon_{zz} = \lambda_z - 1, \quad \varepsilon_{r\theta} = \frac{1}{2}\frac{\mathrm{d}u_\theta}{\mathrm{d}r} - \frac{1}{2r}u_\theta. \tag{45}$$

Using (43) and (45) in (11), we obtain the following system of 4 nonlinear equations:

$$\frac{\mathrm{d}u_r}{\mathrm{d}r} = W_1 + W_2 T_{rr} + W_3\left(T_{rr}^2 + \frac{C_0^2}{r^4}\right), \tag{46}$$

$$\frac{u_r}{r} = W_1 + W_2\left(r\frac{\mathrm{d}T_{rr}}{\mathrm{d}r} + T_{rr}\right) + W_3\left[\left(r\frac{\mathrm{d}T_{rr}}{\mathrm{d}r} + T_{rr}\right)^2 + \frac{C_0^2}{r^4}\right], \tag{47}$$

$$\lambda_z - 1 = W_1 + W_2 T_{zz} + W_3 T_{zz}^2, \tag{48}$$

$$\frac{1}{2}\left(\frac{\mathrm{d}u_\theta}{\mathrm{d}r} - \frac{u_\theta}{r}\right) = W_2\frac{C_0}{r^2} + W_3\frac{C_0}{r^2}\left(2T_{rr} + r\frac{\mathrm{d}T_{rr}}{\mathrm{d}r}\right). \tag{49}$$

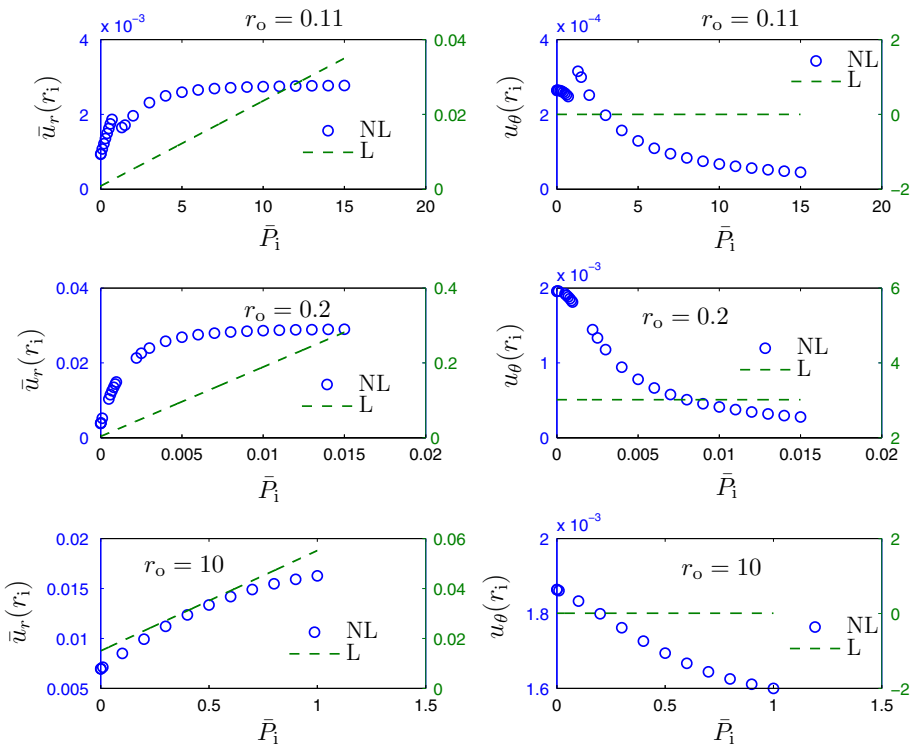

Fig. 14 Tube under the influence of circumferential shear, axial stretch and radial normal stress applied on the inner surface $r = r_i$. Influence of the radial normal stress $\bar{P}_i$ on the dimensionless radial component of the displacement $\bar{u}_r = \frac{u_r}{r}$, and the θ component of the displacement field u_θ, which are evaluated at $r = r_i$. A comparison is presented between the results obtained for a linearized elastic body (L) [see (14) and also note the scale on the right for each plot], and the nonlinear model (NL) [see (13) and also note the scale on the left for each plot]. The radii $r_o = 0.11$; 0.2; 10 m indicate the three different tubes considered (see Table 3)

Regarding the boundary conditions, as in Sect. 3, we consider two cases:

$$\text{(A)}: \quad T_{rr}(r_i) = -P_i, \quad u_r(r_o) = 0, \quad u_z(r_o) = 0, \tag{50}$$

$$\text{(B)}: \quad T_{rr}(r_i) = -P_i, \quad T_{rr}(r_o) = 0, \quad u_z(r_o) = 0. \tag{51}$$

We study the effect of P_i, C_0 and λ_z on the displacements, strains, and stresses.

If we consider the constitutive equation for a linearized elastic body (14), from (46)–(49) for Case (A) we obtain the following exact solutions (see Chapter XIV of [48]):

$$T_{rr} = -\frac{\left\{E(r_i^2 - r^2)r_o^2(\lambda_z - 1)\nu + P_i r_i^2[r^2 + r_o^2(1 - 2\nu)](1 + \nu)\right\}}{r^2[r_i^2 + r_o^2(1 - 2\nu)](1 + \nu)}, \tag{52}$$

$$T_{\theta\theta} = -\frac{\left\{E(r^2 + r_i^2)r_o^2(1 - \lambda_z)\nu + P_i r_i^2(1 + \nu)[r^2 + r_o^2(2\nu - 1)]\right\}}{r^2[r_i^2 + r_o^2(1 - 2\nu)](1 + \nu)}, \tag{53}$$

$$T_{zz} = -\frac{\left\{2P_i r_i^2\nu(1 + \nu) + E(1 - \lambda_z)[r_i^2(1 + \nu) - r_o^2(\nu - 1)]\right\}}{[r_i^2 + r_o^2(1 - 2\nu)](1 + \nu)}, \tag{54}$$

$$u_r = \frac{r_i^2(r^2 - r_o^2)[E(1 - \lambda_z)\nu + P_i(2\nu^2 + \nu - 1)]}{Er[r_i^2 + r_o^2(1 - 2\nu)]}, \quad u_\theta = \frac{C_0(r^2 - r_o^2)(1 + \nu)}{Err_o^2}, \tag{55.1,2}$$

while in the case of the boundary conditions defined as Case (B) we obtain:

$$T_{rr} = \frac{P_i r_i^2(r_o^2 - r^2)}{r^2(r_i^2 - r_o^2)}, \quad T_{\theta\theta} = -\frac{P_i r_i^2(r_o^2 + r^2)}{r^2(r_i^2 - r_o^2)}, \quad T_{zz} = E(\lambda_z - 1) - \frac{2P_i r_i^2\nu}{(r_i^2 - r_o^2)}, \tag{56}$$

$$u_r = \frac{\left\{Er^2(r_i^2 - r_o^2)(1 - \lambda_z)\nu + P_i r_i^2(1 + \nu)[r^2(2\nu - 1) - r_o^2]\right\}}{Er(r_i^2 - r_o^2)}, \tag{57}$$

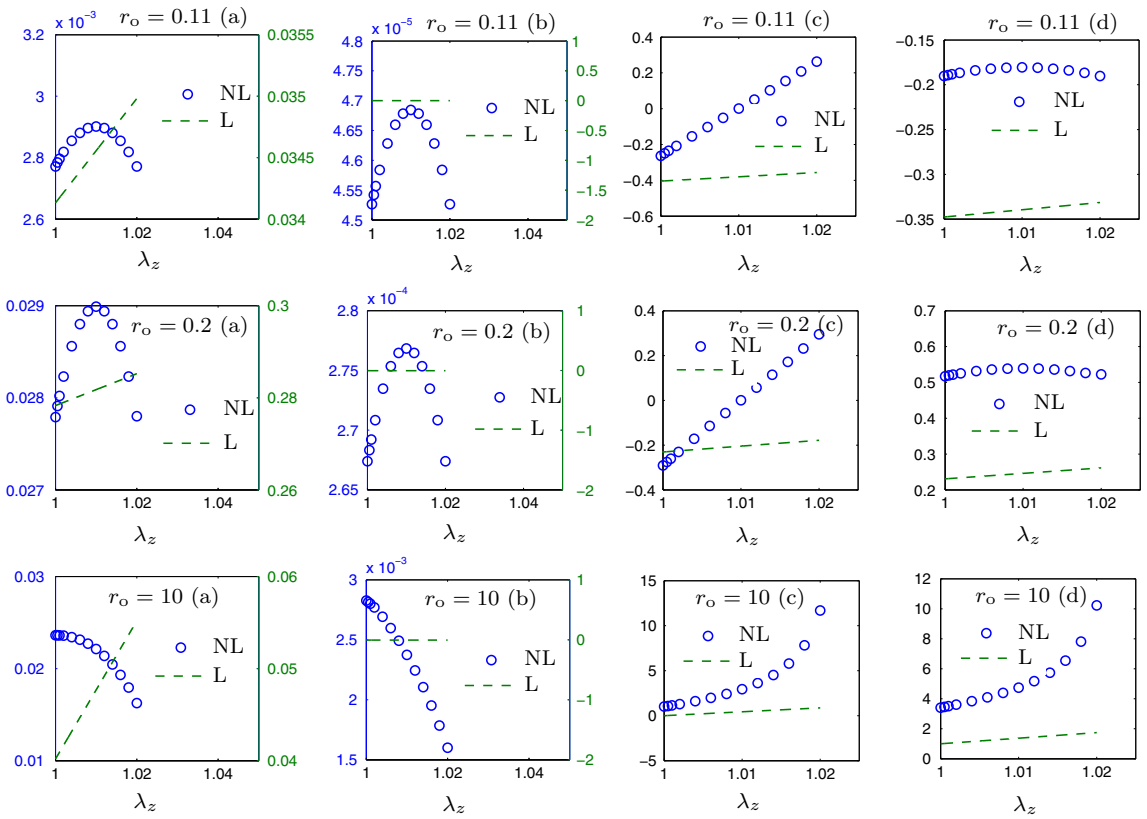

Fig. 15 Tube under the influence of circumferential shear, axial stretch, and radial normal stress applied on the inner surface $r = r_i$. Influence of the stretching λ_z on the dimensionless radial displacement $\bar{u}_r = \frac{u_r}{r_i}$ portrayed as (**a**), on the θ component of the displacement field u_θ depicted in (**b**), on the axial dimensionless component of the stress $\bar{T}_{zz} = \frac{T_{zz}}{P_i}$ provided in (**c**), and the dimensionless component of the stress $\bar{T}_{\theta\theta} = \frac{T_{\theta\theta}}{P_i}$ presented in (**d**). A comparison is provided between the results for considering linearized elastic bodies (L) [see (14)], and the nonlinear model (NL) [see (13)]. The radii $r_o = 0.11$; 0.2; 10 m indicate the three different tubes considered (see Table 3)

and the expression for $u_\theta(r)$ is the same as in (55.2).

When we work with the new nonlinear class of elastic bodies (13), Eqs. (46)–(49) subject to the boundary conditions (50), (51) can be solved numerically. We use the finite element method, and for brevity, we do not discuss the details of the procedure as they have been discussed previously.

Three examples are considered for the tube, where the external radii are different, but with the same internal radius $r_i = 0.1$ m. These three cases are presented in Table 3.
For each case, we list the maximum radial normal stress that was possible for us to apply without having problems with the convergence of the numerical scheme.

In the different plots that are presented, we consider the same dimensionless quantities documented in (41.1–5) and

$$\bar{C}_0 = \frac{C_0}{r_i^2 P_i}, \quad \bar{P}_i = \frac{1}{\bar{C}_0}. \tag{58}$$

In Fig. 12, we present results for the $T_{\theta\theta}$ component of the stress and the radial displacement for the tube, evaluated at $r = r_i$, for the three tubes presented in Table 3 (Case A), versus the natural logarithm of the degrees of freedom.

In Fig. 13, we study the influence of the parameter C_0 [see (43)] on the radial and the θ components of the displacement, which are evaluated at $r = r_i$, where we compare the results obtained using the linearized constitutive equation (14) and the new class of nonlinear constitutive relations (13), working with the boundary conditions indicated as Case (A) [see (50) and Table 3]. From (55.1) it is easy to see that $u_r(r)$ is constant in terms of C_0 in the case of linearized isotropic bodies (14), but there is a slight influence of C_0 on $\bar{u}_r$ for the new class of elastic bodies (13).

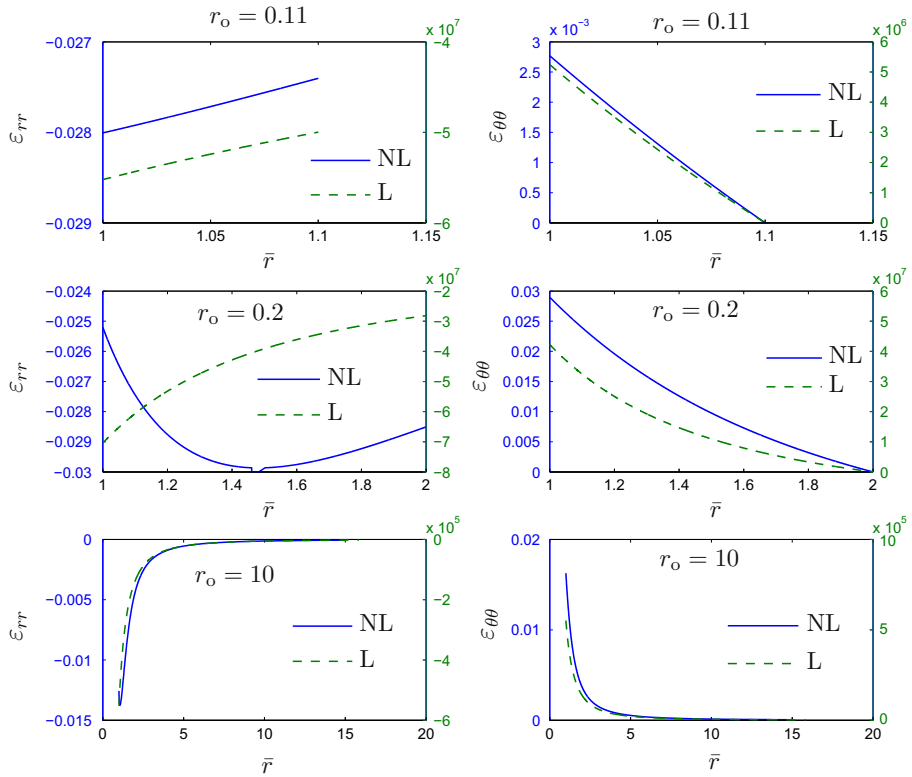

Fig. 16 Tube under the influence of circumferential shear, axial stretch and radial normal stress applied at the inner surface $r = r_i$. Results for the radial and θ components of the strain tensor for the boundary conditions indicated as Case (A) [see (50) and Table 3], for the constitutive equation (14) for linearized elastic bodies (L), and the nonlinear model [see (13)] (NL), versus the dimensionless radius $\bar{r} = \frac{r}{r_i}$. The radii $r_o = 0.11; 0.2; 10$ m indicate the three different tubes considered. For the tube $r_o = 10$ m results are presented for a limited range of $\bar{r}$

In the case of $u_\theta(r)$ from (55.2), we see that for linearized isotropic elastic bodies (14), u_θ depends linearly on C_0, as can be noted from the same Fig. 3. Approximately the same relationship can be observed for the new class of elastic bodies (13).

In Fig. 14, we study the effect of P_i on the radial and θ components of the displacement field, which are evaluated at $r = r_i$, for the nonlinear and linearized constitutive relations defined respectively by (14) and (13). From (55) it is easy to see that u_r depends linearly on P_i and that u_θ is constant (as a function of such a radial normal stress) for linearized elastic bodies (14). That is not the case when working with the nonlinear model (13), as can be observed from the same plots.

To the problem that was considered, we add an axial stretching λ_z to the tube, and in Fig. 15, we present results wherein we study the influence of the parameter with regard to the solution for the problem. We have assumed that $r_o = 0.11; 0.2;$ 10(a) portrays the results for $\bar{u}_r = \frac{u_r}{r_i}$ evaluated at $r = r_i$, for the boundary conditions defined as Case (A) in Table 3. Similar results are presented for u_θ wherein we have assumed that $r_o = 0.11; 0.2;$ 10(b), for $\bar{T}_{zz} = \frac{T_{zz}}{P_i}$ and $\bar{T}_{\theta\theta} = \frac{T_{\theta\theta}}{P_i}$ (see the other plots corresponding to $r_o = 0.11; 0.2;$ 10(c) and $r_o = 0.11; 0.2;$ 10(d), respectively). For linearized elastic bodies (L) (14), from (55), we see that u_r depends linearly on λ_z, while u_θ is constant with regard to that parameter, as can be observed from Fig. 15, which is not the case when working with (13). From (53), (54) we notice that T_{zz} and $T_{\theta\theta}$ depend linearly on λ_z for linearized elastic bodies (14), but the response is nonlinear when working with (13).

The results presented in Fig. 16 are interesting and worth discussing in some detail. In that figure, we have results for the components of the strain tensor, for the boundary conditions indicated as Case (A) (see Table 3), using the linearized constitutive equation (14), and the new class of constitutive relations (13), as functions of the dimensionless radius $\bar{r} = \frac{r}{r_i}$. We notice that the strains are excessively large for the linearized elastic bodies (L), which once again contradicts the basic assumptions under which the approximation is derived, whereas for the new class of elastic bodies (13), the strains remain small in all the cases considered.

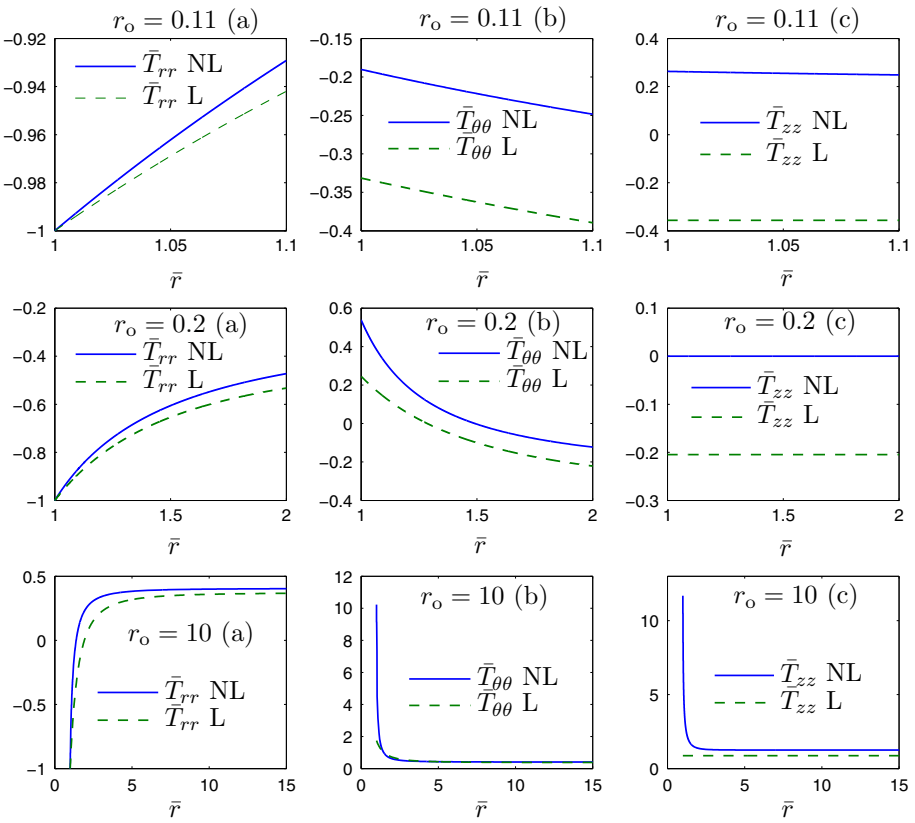

Fig. 17 Tube under the influence of circumferential shear, axial stretch and radial normal stress applied at the inner surface $r = r_i$, for the boundary conditions indicated as Case (A) [see (50) and Table 3]. Results for the dimensionless radial, θ and axial components of the stress tensor $\bar{T}_{rr} = \frac{T_{rr}}{P_i}$, $\bar{T}_{\theta\theta} = \frac{T_{\theta\theta}}{P_i}$ and $\bar{T}_{zz} = \frac{T_{zz}}{P_i}$, respectively, as functions of the dimensionless radius $\bar{r} = \frac{r}{r_i}$. The radii $r_o = 0.11; 0.2;$ 10 m indicate the three different tubes considered (see Table 3). In each plot results are presented for a linearized elastic body [see (14)] (L), and the nonlinear model (13) (NL). For the tube $r_o = 10$ m results are presented for a limited range of $\bar{r}$

Finally, for the boundary conditions indicated as Case (A) (see Table 3), in Figs. 17, 18, we present results for the components of the dimensionless stress tensor $\bar{T}_{rr}$, $\bar{T}_{\theta\theta}$ and $\bar{T}_{zz}$, and the two components of the displacement field $\bar{u}_r$ and u_θ.

In Figs. 19, 20 and 21 we present results for the components of the strain, stress and the displacement fields, for the boundary conditions indicated as Case (B) (see Eq. (51) and Table 3).

5 Concluding remarks

In this paper, we have studied boundary value problems within the context of a new class of elastic bodies described by constitutive relations, wherein the linearized strain depends nonlinearly on the stress. We have picked two boundary value problems that have been studied within the context of the classical linearized constitutive relation, and which admit explicit exact solutions. As the relationship between the stress and the strain is linear, at sufficiently large stresses, the strain becomes large, violating the basic assumption under which the approximate model is derived. On the other hand, for the class of models considered, the strains do not become large enough to violate the assumption under which the linearization is effected. The problems considered are in geometries and loading conditions that have interesting practical relevance. The problems considered are the telescopic shearing and inflation of a cylindrical annulus and the extension and circumferential shear of a cylindrical annulus. Results are presented for two types of boundary conditions, both of which have practical relevance. Unlike the classical problem, one cannot substitute the expression for the stress into the equilibrium equation and obtain a partial differential equation for the displacement field,

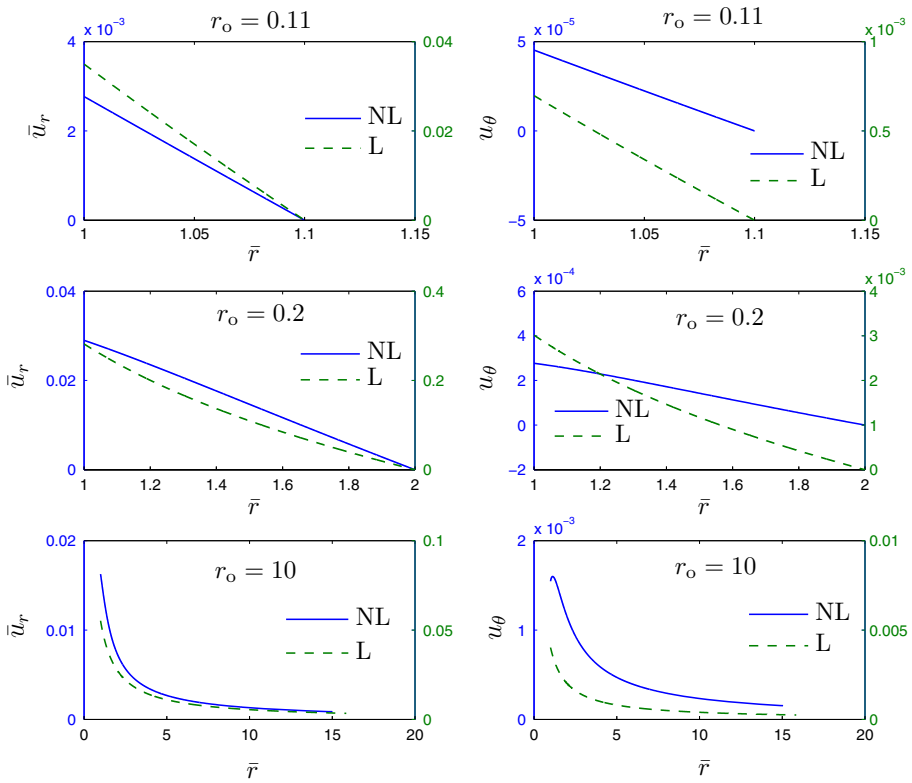

Fig. 18 Tube under the influence of dimensionless shear, axial stretch and radial normal stress on the inner surface $r = r_i$, for the boundary conditions indicated as Case (A) [see (50) and Table 3]. Results for the radial and θ components of the displacement field $\bar{u}_r = \frac{u_r}{r_i}$, u_θ, respectively, as functions of the dimensionless radius $\bar{r} = \frac{r}{r_i}$. The radii $r_o = 0.11$; 0.2; 10 m indicate the three different tubes considered. Results are presented for a linearized elastic body [see (14)] (L), and the nonlinear model (13) (NL). For the tube $r_o = 10$ m results are presented for a limited range of $\bar{r}$

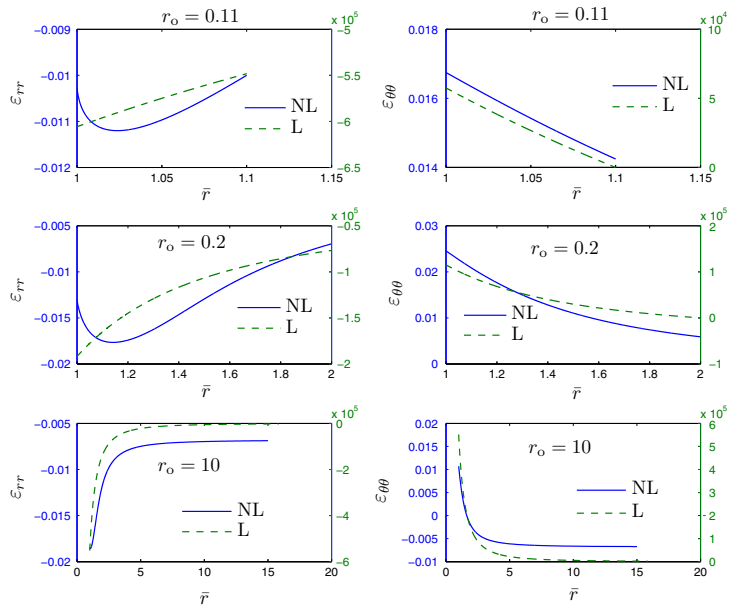

Fig. 19 Tube under the influence of circumferential shear, axial stretch and radial normal stress applied on the inner surface $r = r_i$. Results for the radial and θ components of the strain tensor for the boundary conditions indicated as Case (B) [see (51) and Table 3], for the constitutive equation (14) for linearized elastic bodies (L), and the nonlinear model (13) (NL), versus the dimensionless radius $\bar{r} = \frac{r}{r_i}$. The radii $r_o = 0.11$; 0.2; 10 m indicate the three different tubes considered. For the tube $r_o = 10$ m results are presented for a limited range of $\bar{r}$

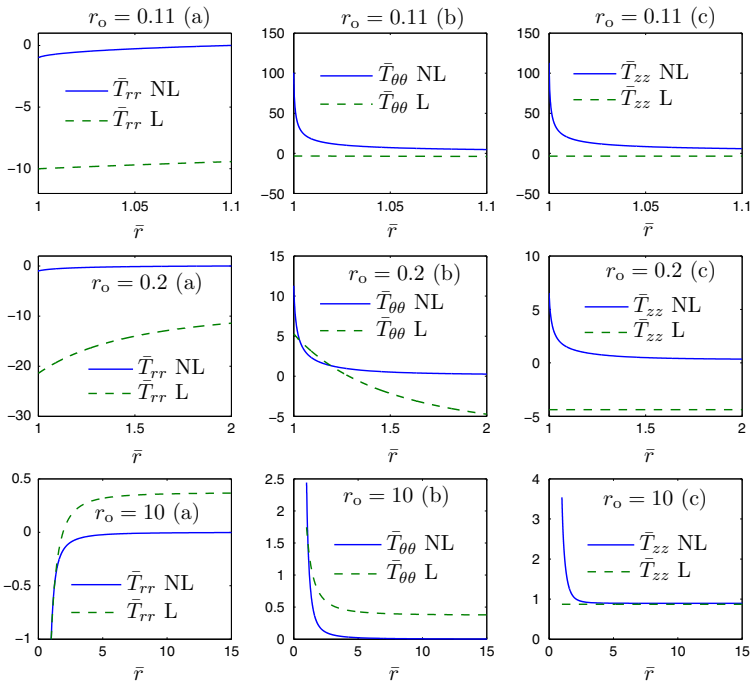

Fig. 20 Tube under the influence of circumferential shear, axial stretch and radial normal stress on the inner surface $r = r_i$, for the boundary conditions indicated as Case (B) [see (51) and Table 3]. Results for the dimensionless radial, θ and axial components of the stress tensor $\bar{T}_{rr} = \frac{T_{rr}}{P_i}$, $\bar{T}_{\theta\theta} = \frac{T_{\theta\theta}}{P_i}$ and $\bar{T}_{zz} = \frac{T_{zz}}{P_i}$, respectively, as functions of the dimensionless radius $\bar{r} = \frac{r}{r_i}$. The radii $r_o = 0.11; 0.2; 10$ m indicate the three different tubes considered. For each plot results are presented for a linearized elastic body [see (14)] (L), and the new nonlinear model (13) (NL). For the tube $r_o = 10$ m results are presented for a limited range of $\bar{r}$

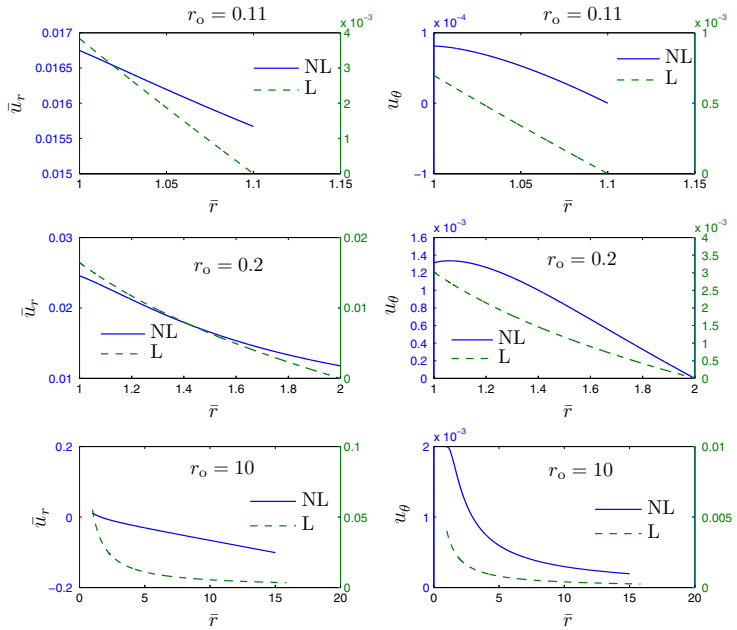

Fig. 21 Tube under the influence of circumferential shear, axial stretch and radial normal stress on the inner surface $r = r_i$, for the boundary conditions indicated as Case (B) [see (51) and Table 3]. Results for the radial and the θ components of the displacement field $\bar{u}_r = \frac{u_r}{r_i}$, u_θ, respectively, as functions of the dimensionless radius $\bar{r} = \frac{r}{r_i}$. The radii $r_o = 0.11; 0.2; 10$ m indicate the three different tubes considered. Results are presented for a linearized elastic body [see (14)] (L), and the nonlinear model (13) (NL). For the tube $r_o = 10$ m results are presented for a limited range of $\bar{r}$

alike the Navier equations for a linearized elastic body. In the case of the nonlinear model considered, one has to solve the strain displacement relation and the constitutive relation simultaneously. This does not accord us the possibility to find exact solutions. The governing equations are solved numerically, and the results are presented in a series of figures that clearly indicate the marked difference between the prediction of the classical linearized elastic model and the nonlinear constitutive relations.

Acknowledgments R. Bustamante would like to express his gratitude for the financial support provided by FONDECYT (Chile) under Grant No. 1120011. K. R. Rajagopal thanks the National Science Foundation and the Office of Naval Research for support of this work.

References

1. Saito, T., Furuta, T., Hwang, J.H., Kuramoto, S., Nishino, K., Susuki, N., Chen, R., Yamada, A., Ito, K., Seno, Y., Nonaka, T., Ikehata, H., Nagasako, N., Iwamoto, C., Ikuhara, Y., Sakuma, T.: Multifunctional alloys obtained via a dislocation-free plastic deformation mechanism. Science **300**, 464–467 (2003)
2. Li, T., Morris, J.W. Jr., Nagasako, N., Kuramoto, S., Chrzan, D.C.: 'Ideal' engineering alloys. Phys. Rev. Lett. **98**, 105503 (2007)
3. Talling, R.J., Dashwood, R.J., Jackson, M., Kuramoto, S., Dye, D.: Determination of C_{11}–C_{12} in Ti–36Nb–2Ta–3Zr–0.3O (xt.%) (Gum metal). Scr. Mater. **59**, 669–672 (2008)
4. Withey, E., Jim, M., Minor, A., Kuramoto, S., Chrzan, D.C., Morris, J.W. Jr.: The deformation of 'Gum Metal' in nanoindentation. Mater. Sci. Eng. A **493**, 26–32 (2008)
5. Zhang, S.Q., Li, S.J., Jia, M.T., Hao, Y.L., Yang, R.: Fatigue properties of a multifunctional titanium alloy exhibiting nonlinear elastic deformation behavior. Scr. Mater. **60**, 733–736 (2009)
6. Rajagopal, K.R.: On implicit constitutive theories. Appl. Math. **48**, 279–319 (2003)
7. Bustamante, R.: Some topics on a new class of elastic bodies. Proc. R. Soc. A **465**, 1377–1392 (2009)
8. Rajagopal, K.R.: Conspectus of concepts of elasticity. Math. Mech. Solids **16**, 536–562 (2011)
9. Guyer, R.A., Johnson, P.A.: Nonlinear mesoscopic elasticity: evidence for a new class of materials. Phys. Today **52**, 30–36 (1999)
10. Johnson, P.A., Rasolfosaon, P.N.J.: Manifestation of nonlinear elasticity in rock: convincing evidence over large frequency and strain intervals from laboratory studies. Nonlinear Process. Geophys. **3**, 77–88 (1996)
11. Lu, Z.: Role of hysteresis in propagation acoustic waves in soils. Geophys. Res. Lett. **32**, L14302 (2005)
12. McCall, K.R., Guyer, R.A.: Equation of state and wave propagation in hysteretic nonlinear elastic materials. J. Geophys. Res. **99**, 23887–23897 (1994)
13. Ostrovsky, L.A.: Wave processes in media with strong acoustic nonlinearity. J. Acoust. Soc. Am. **90**, 3332–3337 (1991)
14. Popovics, S., Rose, J.L., Popovics, J.S.: The behavior of ultrasonic pulses in concrete. Cem. Concr. Res. **20**, 259–270 (1990)
15. Rajagopal, K.R: The elasticity of elasticity. Z. Angew. Math. Phys. **58**, 309–317 (2007)
16. Rajagopal, K.R: On the nonlinear elastic response of bodies in the small strain range. Acta Mech. **225**, 1545–1553 (2014)
17. Green, G.: On the laws of reflexion and refraction of light at the common surface of two non-crystallized media. Proc. Camb. Philos. Soc. **7**, 1–24 (1838). See also pp. 245–269 of *Mathematical papers of the late George Green*, Ed. N. M. Ferris, MacMillan and Company, London (1871)
18. Green, G.: On the propagation of light in crystallized media. Trans. Camb. Philos. Soc. **7**, 121-140 (1839-1842). See also pp. 293–311 of *Mathematical papers of the late George Green*, Ed. N. M. Ferris, MacMillan and Company, London (1871)
19. Carroll, M.M.: Must elastic materials be hyperelastic?. Math. Mech. Solids **14**, 369–376 (2005)
20. Truesdell, C.A., Noll, W.: The non-linear field theories of mechanics. In: Antman, S.S. (ed.), 3rd edn. Springer, Berlin (2004)
21. Rajagopal, K.R, Srinivasa, A.R.: On the response of non-dissipative solids. Proc. R. Soc. A **463**, 357–367 (2007)
22. Rajagopal, K.R, Srinivasa, A.R.: On a class of non-dissipative solids that are not hyperelastic. Proc. R. Soc. A **465**, 493–500 (2009)
23. Bridges, C., Rajagopal, K.R.: Implicit constitutive models with a thermodynamic basis: a study of stress concentration. Z. Angew. Math. Phys. doi:10.1007/s00033-014-0398-5
24. Bustamante, R., Rajagopal, K.R.: A note on plain strain and stress problems for a new class of elastic bodies. Math. Mech. Solids **15**, 229–238 (2010)
25. Bustamante, R., Rajagopal, K.R.: Solutions of some simple boundary value problems within the context of a new class of elastic materials. Int. J. Nonlinear Mech. **46**, 376–386 (2011)
26. Bustamante, R., Rajagopal, K.R.: On the inhomogeneous shearing of a new class of elastic bodies, Math. Mech. Solids **17**, 762–778 (2012). doi:10.1177/1081286511429994
27. Rajagopal, K.R: On a new class of models in elasticity. Math. Comput. Appl. **15**, 506–528 (2010)
28. Freed, A.D.: Soft Solids: A Primer to the Theoretical Mechanics of Materials. Birkhäuser (2014)
29. Rajagopal, K.R., Walton, J.R.: Modeling fracture in the context of strain-limiting theory of elasticity: a single anti-plane crack. Int. J. Fract. **169**, 39–48 (2011)
30. Gou, K., Muddamallappa, M., Rajagopal, K.R., Walton, J.R.: Modeling fracture in the context of a strain limiting theory in elasticity: a single plane-strain crack. Int. J. Eng. Sci. doi:10.1016/j.ijengsci.2014.04.018
31. Ortiz, A., Bustamante, R., Rajagopal, K.R.: A numerical study of a plate with a hole for a new class of elastic bodies. Acta Mech. **223**, 1971–1981 (2012). doi:10.1007/s00707-012-0690-4
32. Ortiz-Bernardin, A., Bustamante, R., Rajagopal, K.R.: A numerical study of elastic bodies that are described by constitutive equations that exhibit limited strains. Int. J. Solids Struct. **51**, 875–885 (2014)

33. Kulvait, V., Malek, J., Rajagopal, K.R.: Anti-plane stress state of a plate with a V-notch for a new class of elastic solids. Int. J. Fract. **179**, 59–73 (2013)
34. Kannan, K., Rajagopal, K.R., Saccomandi, G.: Unsteady motions of a new class of elastic solids. Wave Motion **51**, 833–843 (2014)
35. Kambapalli, M., Kannan, K., Rajagopal, K.R.: Circumferential stress waves in a nonlinear elastic cylinder. Q. J. Mech. Appl. Math. **67**, 193–203 (2014). doi:10.1093/qjmam/hbu003
36. Bustamante, R., Sfyris, D.: Direct determination of stresses from the stress wave equations of motion and wave propagation for a new class of elastic bodies. Math. Mech. Solids **20**, 80–91 (2015). doi:10.1177/1081286514543600
37. Freed, A.D., Einstein, D.R.: An implicit elastic theory for lung parenchyma. Int. J. Eng. Sci. **62**, 31–47 (2013)
38. Criscione, J.C., Rajagopal, K.R.: On the modeling of the non-linear response of soft elastic bodies. Int. J. Nonlinear Mech. **56**, 20–24 (2013)
39. Penn, R.W.: Volume changes accompanying the extension of rubber. J. Rheol. **14**, 509–517 (1970)
40. Bustamante, R., Rajagopal, K.R.: On a new class of electroelastic bodies: part I. Proc. R. Soc. A **469**, 20120521 (2013)
41. Bustamante, R., Rajagopal, K.R.: On a new class of electroelastic bodies: part II. Boundary value problems. Proc. R. Soc. A **469**, 20130106 (2013)
42. Chadwick, P.: Continuum Mechanics: Consice Theory and Problems. Dover Publications INC, Mineola New York (1999)
43. Truesdell, C.A., Toupin, R. (1960) The classical field theories. In: Flügge, S. (ed.) Handbuch der Physik, Vol. III/1. Springer, Berlin
44. Saada, A.S.: Elasticity: theory and application. Krieger Publishing Company, Malabar Florida (1993)
45. Rajagopal, K.R: A note on material symmetry for bodies defined by implicit constitutive relations. (Submitted)
46. Karra, S., Rajagopal, K.R.: Development of three dimensional constitutive theories based on lower dimensional data. Appl. Math. **54**, 147–176 (2009)
47. Rajagopal, K.R, Srinivasa, A.R.: On the use of compatibility equations for the strain in linear and non-linear theories of mechanics. Math. Mech. Solids. doi:10.1177/1081286513509506
48. Lamé, M.G.: Leşons sur la Théorie Mathématique de L'Élasticité des Corps Solides. Deuxième Édition, Paris, Gauthier-Villars (1866)
49. Comsol Multiphysics, Version 3.4, Comsol Inc. Palo Alto, CA, (2007)